A Novel Role for *Lunatic Fringe* in the Development of Epaxial Musculature

by

Corinne De Ruiter

A Thesis Presented in Partial Fulfillment
of the Requirements for the Degree
Master of Science

Approved April 2012 by the
Graduate Supervisory Committee:

Jeffery Rawls, Chair
Kenro Kusumi
Jeanne Wilson-Rawls
Rebecca Fisher

ARIZONA STATE UNIVERSITY

May 2012

ABSTRACT

Skeletal muscles arise from the myotome compartment of the somites that form during vertebrate embryonic development. Somites are transient structures serve as the anlagen for the axial skeleton, skeletal muscle, tendons, and dermis, as well as imposing the metameric patterning of the axial musculoskeletal system, peripheral nerves, and vasculature. Classic studies have described the role of Notch, Wnt, and FGF signaling pathways in controlling somite formation and muscle formation. However, little is known about the transformation of myotome compartments into identifiable post-natal muscle groups. Using a mouse model, I have undertaken an evaluation of morphological events, including hypertrophy and hyperplasia, related to the formation of several muscles positioned along the dorsal surface of the vertebrae and ribs. *Lunatic fringe* (*Lfng*) deficient embryos and neonates were also examined to further understand the role of the Notch pathway in these processes as it is a modulator of the Notch receptor and plays an important role in defining somite borders and anterior-posterior patterning in many vertebrates. *Lunatic fringe* deficient embryos showed defects in muscle fiber hyperplasia and hypertrophy in the iliocostalis and longissimus muscles of the erector spinae group. This novel data suggests an additional role for *Lfng* and the Notch signaling pathway in embryonic and fetal muscle development.

DEDICATION

I would like to dedicate this Master's thesis to my late grandfather, Bill Caylor, who initiated my interest and passion for science.

ACKNOWLEDGMENTS

I would like to acknowledge the inspiration and guidance provided by my mentor, Dr. Alan Rawls, and the continued support of past and present members of the Rawls and Wilson-Rawls labs. I would also like to acknowledge the support from my family, especially my father, Robert DeRuiter, and my step-mother, Kristi Lattin, for always encouraging me to push myself and continue my education. Additionally I'd like to thank my mother, Donna Caylor, my grandmother, Marie Caylor, and my sister, Hannah Fricke for cheering me on, and inspiring me to complete this process. Lastly, I'd like to acknowledge Brad Jacobson, for providing me with an unimaginable amount of support, for enduring this process with me, and for sharing my love and passion for science.

TABLE OF CONTENTS

LIST OF TABLES

LIST OF FIGURES

CHAPTER 1

INTRODUCTION

The vertebrate body plan is characterized by a segmental organization that is reflected in the axial skeleton, skeletal muscle, peripheral nerves, and vasculature along the anterior/posterior axis. This patterning is imposed by the transient formation of somites on either side of the neural tube during embryogenesis. Each somite contains the anlagen for the skeleton and muscle which undergoes significant cell migration to form the functional elements of the musculoskeletal system. The past two decades have seen considerable advances in our understanding of how canonical signaling pathways, including the Notch, Wnt, FGF, and TGF-ß pathways, intersect in the initiation of skeletal muscle specification and differentiation within individual somites. However, little is known about how the formation of functional skeletal muscles is regulated during embryonic and fetal development.

The process by which skeletal muscles develop is obscured by the fact that each somite contributes to multiple muscles and that myogenesis occurs in several waves of formation. In the current study, we focused on the development of epaxial muscles as they do not migrate away from the somite region, are segmented, and span multiple vertebral levels. The adult placement of epaxial muscles is intimately related to the progenitor cell population within the somites along the anterior/posterior axis. This analysis focused on the iliocostalis that extends from the ilium or a transverse process and inserts on a more cranial transverse process or rib and the longissimus, a

columnar muscle that extends from either the ilium or a transverse process, and inserts on a more cranial transverse process, rib, atlas, or the occipital. We determined the positioning of these epaxial muscles in wild type embryos as well as embryos that lacked the *Lunatic fringe* (*Lfng*) gene in E15.5 through neonatal mice. We chose to analyze epaxial muscles in the *Lfng*$^{-/-}$ because *Lfng* is a modifier of the Notch signaling cascade which has been identified in many developmental processes including myogenesis. Epaxial muscular defects have been identified in the Notch mutants Lfng$^{-/-}$ and Dll3$^{-/-}$ (Fisher 2011; Fisher et al. 2012), however whether they arise from disruption of embryonic muscle development or atrophy due to muscle disuse secondary to vertebral and rib defects, has yet to be determined.

Somitogenesis

Somites are derived from rods of paraxial mesoderm, called presomitic mesoderm (PSM),that lie on either side of the neural tube at the posterior end of vertebrate embryos. Somites form through the synchronous pinching off of cells at the anterior end of the PSM (Figure 1). The first somites to form will give rise to the occipital bone of the skull and the associated skeletal muscle. Through the sequential addition of new somites, the cells required for the formation of the skeletal and muscle elements at the cervical, thoracic, lumbar, sacral and caudal levels are laid down. Creating a distinct boundary between newly formed somites and the anterior PSM is associated with a transition of cells from a mesenchymal to epithelial morphology (MET) (Kalcheim and Ben-Yair 2005; Ordahl and Le Douarin 1992). Cells in the

PSM adopt an anterior/posterior axis that will provide cells within individual somites with a spatial identity. The combination of these events is necessary for the positional information for the segmental patterning of nerves and blood vessels to form that later play a role in directing muscle patterning and adult function (Kalcheim and Ben-Yair 2005; Ordahl and Le Douarin 1992).

The cyclical, synchronous nature of somite formation reveals the existence of a segmental clock that controls the timing of somitogenesis. This is exemplified in the mouse embryo by the consistent formation of new somites every 120 minute intervals between embryonic days E7.75 and E13.5 (Stauber et al. 2009). A clock and wavefront model, initially proposed by Cooke and Zeeman, hypothesized a mechanism of imposing positional information of the new somite boundary in the anterior presomitic mesoderm while integrating with an oscillating signal that dictates the timing of somite formation (Cooke and Zeeman 1976). Though the original model was largely theoretical, genes have been identified that fit within this model, including a deterministic wavefront created by FGF8. (Yamaguchi et al. 1992; Sawada et al. 2001; Dubrulle and Pourquié 2004). The Notch and Wnt signaling pathways have been shown to play a driving force of the segmentation clock (Pourquié 2002). For example, many members of the Hairy/ enhancer of split (*Hes)* family of genes, the glycosyltransferase *Lunatic fringe*, and the Notch ligand, DeltaC are all related to the Notch signaling pathway, and all are cyclically expressed in the PSM during somitogenesis (reviewed in Pourquié 2003). Further investigation into the role of these cyclic genes has revealed that *her1* and *her2* (*Hes* genes in the zebrafish) regulate their own expression

by way of a negative feedback loop. *Lfng* is activated by *Notch1* in a negative feedback loop that leads to Notch inhibition (Dale et al. 2003). *Lfng* deficient embryos cannot inhibit *Notch1*, leading to constitutively active Notch in the PSM (Morimoto et al. 2005). However, constitutively expressing *Lfng* in the PSM does not collapse the cyclical expression of itself or *Hes7*, suggesting *Lfng* is not the only molecule required for Notch signaling (Serth 2003; Kusumi and Dunwoodie 2010).

The Wnt signaling molecule, *Axin2,* also shows cyclical expression in the PSM during somitogenesis, again by way of a negative feedback loop (Aulehla 2004). However, *Axin2* deficient embryos do not show any mutant somite phenotype suggesting that Wnt plays a role in the segmentation clock, but it is not part of any master control mechanism (Yu et al. 2005). FGF pathway components also oscillate, many in phase with Notch components, during somitogenesis. Those genes include *Snail*, *Snai2*, and *Dusp4* (Kusumi and Dunwoodie 2010). *Fgf8* signaling is also involved in somite size and its expression peaks at the posterior end of the embryo (Aulehla 2004). Although they are not direct controllers of the segmentation clock, Wnt and FGF signaling molecules define the determination front, which determines expression of segmentation and myogenic differentiation genes.

Mutations that affect the anterior/posterior axis of somitic mesoderm can be split into two groups: those that are attributed to the Wnt/FGF pathway and those attributed to the Notch signaling pathway. In Wnt/FGF mutants, posterior paraxial mesoderm does not form and in Notch mutants the posterior paraxial mesoderm does not properly segment (Pourquié 2001).

Notch1, *Rbpj (RBPjk)*, *Mesp2*, *Dll1*, *Dll3*, and *Lfng* are all within the Notch group of mutations while *Fgfr1a*, *T (Brachyury)*, *Tbx6*, *Wnt3a*, *Tcf1*/*Lef1*, and *Itga5* (*Integrin* α5) are all examples of the Wnt/FGF pathway mutations (Pourquié 2001). All of these mutations result in somites that are either improperly formed or unsegmented and lead to a disrupted pattern of somite-derived structures.

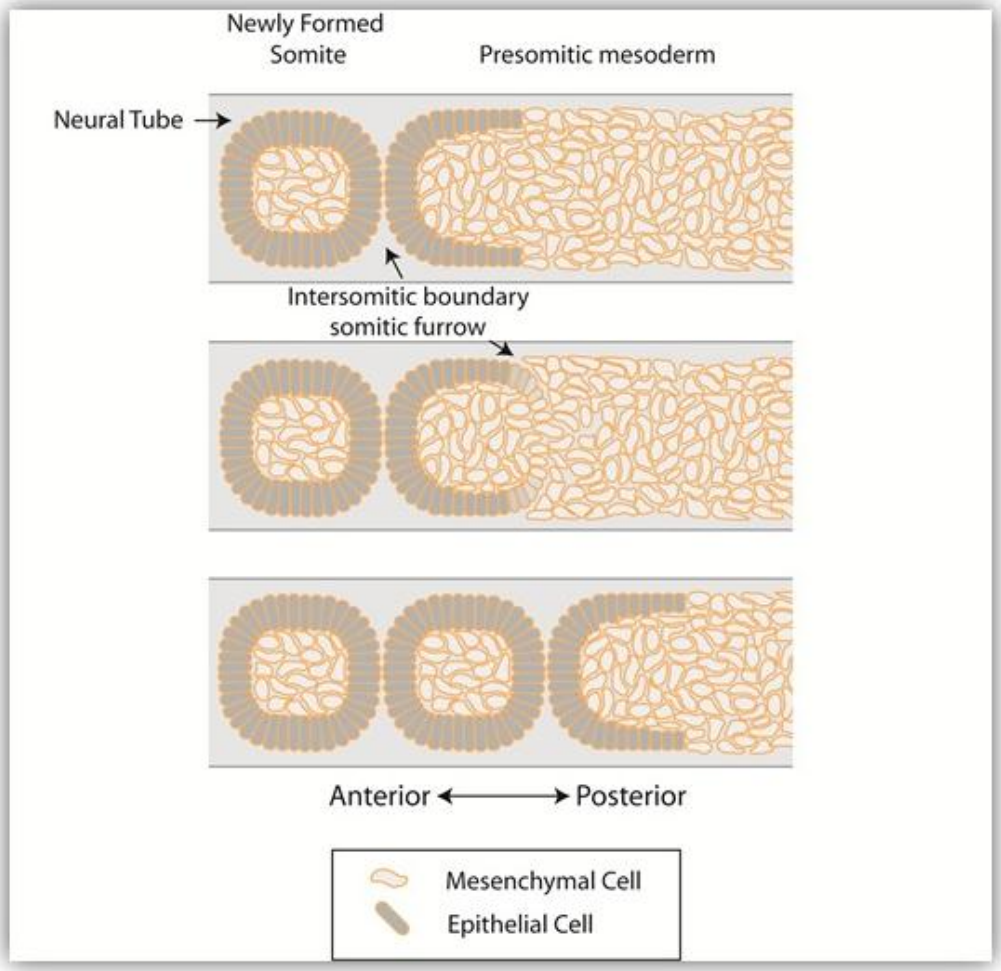

Fig. 1 Somite Formation. The anterior most region of the PSM buds off to form a new somite. This is achieved by a mesenchymal to epithelial transition and formation of the somitic furrow.

Somite Maturation and Myotome Formation

Somites form as epithelial balls with a mesenchymal cell filled somitocoele that lie on either side of the neural tube just below the ectoderm (Figure 2A). The epithelial somite will ultimately give rise to four distinct cellular compartments – sclerotome, syndetome, myotome and dermomyotome, which give rise to the skeleton, tendons, skeletal muscle, and dermis, respectively. After initial segmentation from the PSM, the ventral region of the somite undergoes a transition from epithelial cells to mesenchymal cells (EMT) in which the cells take on a more unorganized morphology for increased cell-cell contact. The newly formed mesenchymal cells differentiate into the sclerotome, and later syndetome, while the dorsal most region of the somite remains epithelial (Figure 2B). This epithelial region of the somite, called the dermomyotome, will also undergo an EMT. Cells from the dorsomedial lip (DML) and ventrolateral lip (VLL) of the dermomyotome will migrate subjacently to form the epaxial and hypaxial myotome, respectively (Figure 2C and 2D). The DML cells are the first to migrate in the embryo, followed by the VLL cells. The myotome will give rise to myogenic precursor cells committed to the myogenic lineage (Stockdale 1992). Cells from the myotome will form muscle by either continuing to mature in the axial region of the embryo or migrating out to the limbs and body wall.

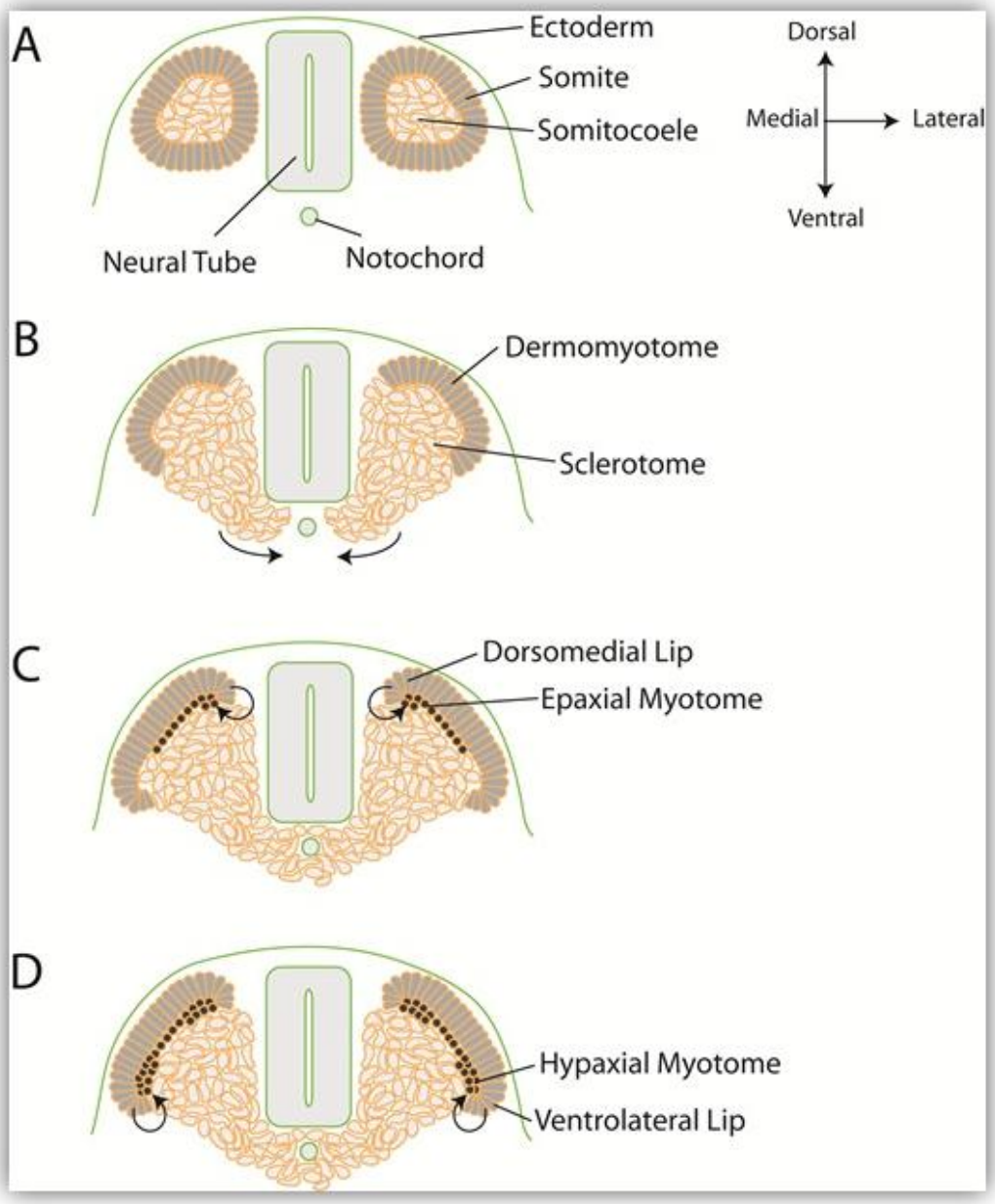

Fig 2. Somite Maturation. Somites form on either side of the neural tube, just below the ectoderm (A). The ventral region somite undergoes an EMT, to become sclerotome, while the dorsal region remains epithelial, becoming dermomyotome (B). Cells from the DML of the dermomyotome migrate to form the epaxial myotome (C), followed by another cell migration from the VLL, which forms the hypaxial myotome (D).

Myotome formation has been hypothesized to form solely by cells migrating from the dorsal medial lip of the dermomyotome or by a combination cells of the myotome form from the DML as well as the region along the ventrolateral extent of the dermomyotome (Hollway and Currie 2003; Ordahl et al. 2001; Kahane et al. 1998a, b). Those two explanations have led to two different models of myotome formation.

Ordahl and colleagues suggest that the primary myotome forms from a translocation and elongation of cells from the DML and VLL that are gradually replaced by new myoblasts (Hollway and Currie 2003; Ordahl et al. 2001). The formation of new myoblasts displaces the older ones leading to the expansion and growth of the myotomal region. In addition to that, the DML remains a source of cells for the dermomyotome giving it stem cell-like properties (Venters and Ordahl 2002). Kalcheim and colleagues state that a wave of cells, called pioneer cells, come from the DML and migrate into the myotomal compartment (Kahane et al. 1998). Next, as the dermomyotome undergoes an epithelial to mesenchymal transition (EMT) an additional group of post-mitotic pioneer cells delaminate and migrate into the most anterior region of the myotome compartment. Those cells then extend from the most anterior region to the most posterior region of each somitic segment. Together, these two morphological events create the myotomal compartment (Kahane et al. 1998a, b; Kalcheim and Ben-Yair 2005).

Once cells are integrated into the myotome, they are committed to the myogenic lineage, which includes myoblasts (progenitor cells), myocytes (muscle cells), satellite cells (progenitor cells for the regeneration of adult

muscle cells), and myofibers (multinucleated and differentiated muscle cells) that will eventually form fully developed muscles. The formation of this embryonic muscle is regulated by signaling pathways associated with the embryonic body plan, such as the Hox family and those linked to lineage-specific specification and differentiation, including the myogenic basic helix-loop-helix (bHLH) transcription factor family (*Myf5, Myod1 (MyoD), Myog (myogenin)* and *Myf6 (MRF4)*), *Mef2a-d*, and members of the Pax and Six gene families (Megeney et al. 1996; Cinnamon et al. 1999; Nowicki and Burke 2000).

Myf5 and *MyoD* are functionally redundant genes required for specification of myogenic progenitor cells to the myogenic lineage. They can be distinguished temporally and spatially in the initiation of their transcription. *Myf5* is expressed in the dorsomedial region of the somite at embryonic day 8.0 (E8.0), where it plays an essential role in the initiation of the corresponding myotome and the muscles derived from it (Braun and Arnold 1996; Kablar et al. 1997; Pownall et al. 2002). In contrast, *MyoD* is first detectable on embryonic day 10.0 (E10.0) in the ventrolateral region of the somite (Kablar et al. 1997; Megeney et al. 1996; Pownall et al. 2002). *MyoD* is important in the formation of the corresponding myotome and the muscle mass in the limb (Kablar et al. 1997; Megeney et al. 1996). The functional redundancy of these genes is underscored by the *MyoD*/*Myf5* knockout there is a complete absence of cells expressing genes in the myogenic lineage (Kablar et al. 1997). In addition to specification, *MyoD* and *Myf5* promote the transcription of *Myogenin*, which is necessary for the

differentiation of myoblasts to form myotubes (Buchberger et al. 1994; Rawls et al. 1995; Pownall et al. 2002).

Members of the Pax family, including *Pax3* and *Pax7*, are also functionally important in muscular development as they activate *MyoD* and *Myf5* ((Relaix et al. 2005; Buckingham 2006). *Pax3* is expressed in many tissues including the dorsal neural tube, cranial neural crest cells, and muscle cells of the body wall and limb bud (Cinnamon et al. 1999; Pownall et al. 2002; Relaix et al. 2005; Bajanca et al. 2004). Without *Pax3* muscles cannot properly develop, especially in the hypaxial regions (Cinnamon et al. 1999; Dietrich 1999; Relaix et al. 2005). *Pax7* is expressed slightly later than *Pax3* and is not as essential for muscle formation as its effects are seen postnatally (Relaix et al. 2005). A double mutation of *Pax3* and *Pax7* results in no trunk muscle formation leading to the conclusion that they work together and are necessary for proper muscle development (Relaix et al. 2005).

Genes such as *Tcf15 (Paraxis)* and *Mesp2* are essential for the development of non-migratory myogenic progenitor cells. *Paraxis* is expressed in the anterior two thirds of the PSM, throughout the epithelial somite, and dermomyotome (Burgess et al. 1996; Wilson-Rawls et al. 1999; Takahashi et al. 2007). *Paraxis* is involved in myogenic specification and without it, muscles form but are severely disrupted (Wilson-Rawls et al. 1999; Takahashi et al. 2007). *Mesp2* is essential for activating the genes *Notch2*, *FGFR1*, *Cer1*, *Epha4*, *Tbx18*, and suppressing *Dll1* and *Uncx* (*Uncx4.1)*, and plays a role in the initial segmentation of somites (Takahashi et al. 2007).

Mesp2 deficient mice display axial skeletal defects, including fused vertebrae and ribs (Saga et al. 1997).

Other genes, such as *Lbx* and *Meox2* are critical for the proper development of migratory myogenic progenitor cells that become the muscles of the limbs and body wall. *Lbx* is co-expressed with *Pax3* in migrating myogenic progenitor cells that will become limb muscles (Pownall et al. 2002). Without *Lbx*, dorsal muscles in the forelimb as well as all muscles in the hindlimb, do not develop (Gross et al. 2000; Buckingham 2001). *Meox2*, is also expressed in the migrating limb bud cells and in paraxial mesoderm (Stamataki et al. 2001). In the *Meox2* mutant, forelimbs are missing muscles and hindlimb muscles are reduced in size (Stamataki et al. 2001).

Classic *Drosophila* studies have shown the importance of homeobox (Hox) genes in segmenting the body and acting as both enhancers and repressors for other genes involved in these processes (McGinnis et al. 1984; Casares et al. 1996). The most prominent feature of the Hox gene family is that the expression pattern along the anterior/posterior axis corresponds to the relative location of the genes on the chromosome (Burke and Nowicki 2001). Hox genes are one of the major players in determining axial identity and global patterning within the developing embryo. Hox genes have been shown to play a role in muscle formation, specifically the homeobox containing gene *Lbx1* which is expressed in migratory muscle precursor cells (MMPs) that later become muscles of the limb, diaphragm, and tongue (Alvares et al. 2003). In addition to that, the Hox10 group in mice was determined to play an important role in vertebrae identity, particularly in

the thoracic to lumbar transition (Carapuco 2005). Defects in Hox genes have been associated with patterning defects along the anterior/posterior axis, including malformation of ribs and fusion of vertebrae, confirming the importance of Hox clusters in initiating body plan development (Carapuco 2005).

Correct somite formation is essential for the global patterning of muscles. This global patterning can be seen at each different axial somite level in which every somite is different from the one directly anterior or posterior to itself (Burke and Nowicki 2001). Somites have intrinsic properties and they receive external signals from surrounding tissue to differentiate differently from one another. This is most likely the case for not only anterior/posterior patterning, but for dorsal/ventral patterning within each somite as well. Although each somite contains cells that will differentiate into myotome, each somite is fated to become a different muscle component than any other somite along the body axis.

Hypaxial and Epaxial Myotome

Skeletal muscles are categorized as epaxial and hypaxial based on their innervation by the dorsal (epaxial) or ventral (hypaxial) rami of the spinal nerves. The myogenic progenitor cells that lie within the myotome of each somite respond to cues from the notochord and from other surrounding tissues allowing them to become fated to either the hypaxial or epaxial cell lineage (Wilson-Rawls et al. 1999; Nowiki 2001; Kardon et al. 2003; Bajanca et al. 2004; Hollway and Currie 2005; Bismuth and Relaix 2010). Both

muscle types are induced by different regions of the somite and surrounding tissues to become fated to their final structures.

Epaxial muscles are deep back muscles that lie dorsal to the vertebral column (Dietrich 1999; Deries et al. 2008). Epaxial muscles are innervated by the dorsal ramus of spinal nerves and evidence suggests that they are innervated later in development than hypaxial muscles (Deries et al. 2008). Epaxial cells are derived from the medial somite and are induced by the neural tube, notochord, and ectoderm (Dietrich 1999). The epaxial myotome is transitory in mammals and is later replaced by the deep back muscles (Deries et al. 2010).

Studies of epaxial muscle development in rat embryos have determined that the muscles of the deep back begin to pattern during embryonic days 12.5 to 15.5 (Deries et al. 2010). The equivalent days in mouse embryogenesis are E11.0 to E14.0. At this stage, the epaxial muscles are underdeveloped and it is not until secondary myogenesis takes place, from about embryonic day 14.5 to 16.5, that the muscles begin to resemble their adult counterparts. In addition to this, epaxial muscles are innervated from E12.5 to E14.0 in rat embryos, after the myotome has already began to transform into the deep muscles of the back (Deries et al. 2008; Deries et al. 2010). Those findings suggest that the epaxial myotome has an intrinsic mechanism for patterning and is not wholly dependent on innervation (Deries et al. 2008).

Epaxial muscles include the erector spinae and transversospinalis groups as well as a deep layer that includes the levators costarum,

intertransversarii, and interspinalis. The erector spinae is composed of three muscle groups that extend from the lumbar vertebrae to the cervical vertebrae and lie on either side of the vertebral column. The erector spinae muscles are, in order from medial to lateral, the spinalis, the longissimus, and the iliocostalis (Cook 1965; Kaufman 1992; Fisher et al. 2012). The transversospinalis muscles function to rotate and extend the vertebral column and are found originating on the transverse process of lumbar and thoracic vertebrae and inserting into the spinous process of adjacent vertebrae (Fisher et al. 2012). The multifidus (most medial), semispinalis (most superficial), and rotatores (most deep) muscles are all part of the transversospinalis group and aid in stabilization (Fisher et al. 2012; Cook 1965; Kaufman 1992).

In the adult, hypaxial muscles are superficially, laterally, and ventrally located (Ordahl and Le Douarin 1992; Dietrich 1999; Christ and Brand-Saberi 2002; Bajanca et al. 2004). Hypaxial cells are derived from the VLL of the dermomyotome and are induced by lateral mesoderm and ectoderm (Dietrich 1999; Bajanca et al. 2004). Wnt signaling from the ectoderm induces precursor cells to become committed to the hypaxial lineage. Hypaxial precursor cells undergo an epithelial-to-mesenchymal transition (EMT) and give rise to muscle in two distinct ways (Ordahl and Le Douarin 1992; Christ and Brand-Saberi 2002; Bajanca et al. 2004). The body wall muscles are formed from non-migratory hypaxial cells and the limb muscles are formed by migratory hypaxial cells (Dietrich 1999). The ventral body wall muscles are formed by the ventrolateral extension of the hypaxial

dermomyotome and limb muscles are formed when migratory precursor cells leave the hypaxial dermomyotome and form muscle masses in the limb buds (Ordahl and Le Douarin 1992; Dietrich 1999; Christ and Brand-Saberi 2002; DeLaurier et al. 2008). Once in the limbs, the cells aggregate and differentiate into dorsal and ventral masses that eventually become specific muscles of the forelimb and hindlimb (Christ et al. 1977; Christ and Brand-Saberi 2002). Hypaxial muscles in the limb bud are immediately innervated upon migration by the ventral rami of spinal nerves (Deries et al. 2008).

Muscle Formation and Growth

Adding to the complex fashion of muscle formation is the fact that myogenesis occurs in two stages: primary and secondary myogenesis. These two stages of myogenesis represent the transition from embryonic muscle to fetal and post-natal muscle. During development, myogenic progenitor cells either self-renew or respond to *Myf5*, *MyoD*, and *Notch* to form myoblasts. This activation and proliferation phase is also negatively regulated by TGF-ß. Myoblasts then fuse to form primary myotubes, a process initiated by *Myogenin* and *Mef2* and inhibited by *Myostatin* and *Notch*. Next, secondary myogenesis is initiated by innervation from newly formed nerves. Secondary myocytes form adjacent to the region where a primary myofiber is innervated, a process also regulated by Notch signaling. Muscle growth is a delicate balance between proliferation, differentiation, and maturation and self-renewal and in general, primary myogenesis is responsible for initiating muscle formation whereas secondary myogenesis is responsible for creating

the bulk of each muscle. Hyperplasia, an increase in the number of muscle fibers, and hypertrophy, an increase in the size of a fiber, are both essential elements of muscle growth and maturation.

Once the muscle is fully formed, the microscopic and intricate network of muscle fibers can be fully appreciated. Each muscle mass is made up of thousands of fibers produced during primary and secondary myogenesis. Each muscle fiber is composed of hundreds to thousands of myofibrils. Calcium is stored in the region surrounding each myofibril, called the sarcoplasmic reticulum (Sandow 1970). Myofibrils are made up of sarcomeres, which are repeated segments of actin and myosin. Myosin is composed of two heavy and two light chains which interact with the actin filaments. Actin filaments are made of the polymer G-actin which forms two strands that twist around each other (Sandow 1970). Muscles are also made up of three different types of fibers: slow twitch (slow oxidative, aerobic, and rich in mitochondria), fast twitch α (fast oxidative, aerobic, rich in mitochondria), and fast twitch ß (fast oxidative, anerobic, and glycolytic) (Sandow 1970). The ratio of the different types of muscle fibers within each muscle group determines the functional characteristics of that muscle group. As an example, slow twitch fibers are used for sustaining muscle use over a long period of time whereas fast twitch fibers are used for short bursts of energy. During primary myogenesis, fast and slow twitch proteins are present, but during secondary myogenesis, only slow twitch proteins are present.

After differentiation and maturation of muscle fibers, the primary muscle masses must become patterned along with the skeletal, vascular, and neuronal elements of the developing body. Muscle patterning is directed by signals produced by adjacent tissues including developing connective tissue, newly formed nerves, and vascularization (Arber et al. 2002). In addition to genetic signals, several morphological processes are involved in the patterning of muscle including splitting, fusion, and migration. The morphological processes coupled with the coordinated development results in embryonic and fetal muscle that assumes the correct shape, location, and fiber orientation.

In muscles such as the rhomboids which lie in the thoracic region of the back attached to the scapula and vertebrae, the direction of muscle fibers changes during development, most likely because their attachment points are simultaneously growing and migrating (Nowiki 2001). Fiber direction change may also be due to the migratory nature of the precursor cells and developing attachment sites. Additionally, smaller muscle segments may fuse into larger muscle groups; for example, the erector spinae muscles remain segmented in the thoracic region of the back but fuse in the lumbar region into one large muscle mass (Nowiki 2001). Fusion events between myogenic cells are essential for the formation of muscle segments in *Drosophila* (Ruiz-Gomez 1998).

Conversely, myotome masses can split to form multiple muscles from one progenitor mass. For instance in humans, both the trapezius and sternocleidomastoid muscles develop by splitting from a single progenitor

muscle mass (Nowiki 2001). In the chick limb bud, it was determined that between stages 24 and 28 pre-muscle masses split to form new muscle masses; however, those masses are not fully patterned until stage 36 (Murray and Wilson 1997). Muscle masses splitting in the chick limb bud leads to the production of 46 individual muscles (Murray and Wilson 1997). Many muscle cells migrate to various destinations in the body during development; the latissimus dorsi forms after muscle cells migrate to cover the superficial surface of the back (Nowiki 2001). Additionally, some muscle cells die via apoptosis and degenerate or convert to connective tissues (McClearn et al. 1995; Nowiki 2001).

Notch Signaling

The Notch pathway is highly conserved across most multicellular organisms and is involved in many processes of development, including neurogenesis, angiogenesis, and cell fate decisions regarding muscle, bone, and organ development (Weinmaster and Kintner 2003). Notch is highly expressed in the presomitic mesoderm (PSM) and displays an oscillatory signal that defines intra- and inter- somitic boundaries (Dale et al. 2003; Aulehla 2004). Notch signaling has been well studied as a candidate for regulating skeletal muscle patterning due to its involvement in somitic patterning, the segmentation clock, cell fate decisions, and proliferation (Ferjentsik et al. 2009; Lewis et al. 2009). A mutation in the Notch signaling pathway or one of its components such as *delta C* in the zebrafish, and *Hes 7* in the mouse commonly results in patterning and segmentation defects of the

vertebrae, ribs, and other somite derived structures (Hollway and Currie 2005). Additionally, Notch signaling has been identified as an inhibitor of myogenesis both through the activation of *HES*-1 and itself (Wilson-Rawls et al. 1999).

Notch signaling begins when Notch, a single-pass transmembrane protein binds to one of its two possible classes of ligands—Jagged/Serrate or Delta (Ferjentsik et al. 2009). When Notch binds to one of those ligands, a portion of Notch called the notch intracellular domain (NICD) is proteolytically cleaved and translocated into the nucleus of the cell (Ferjentsik et al. 2009). Intramembrane proteolysis (RIP) facilitates the cleavage events required to activate Notch by way of presenilin (PS)-dependent gamma-secretase activity (γ-secretase/PS) (Weinmaster and Kintner 2003). In the nucleus, the NICD along with its DNA binding partner, CSL (CBF1, Suppressor of Hairless, Lag-1), act as transcriptional regulators for members of the Hairy/E(sp1) transcription factor family (*Hes* genes) (Hollway and Currie 2005; Pursglove and Mackay 2005; Lewis et al. 2009). Together these components result in a signaling cascade that is important in specification of many embryonic tissues, diagramed in Figure 3.

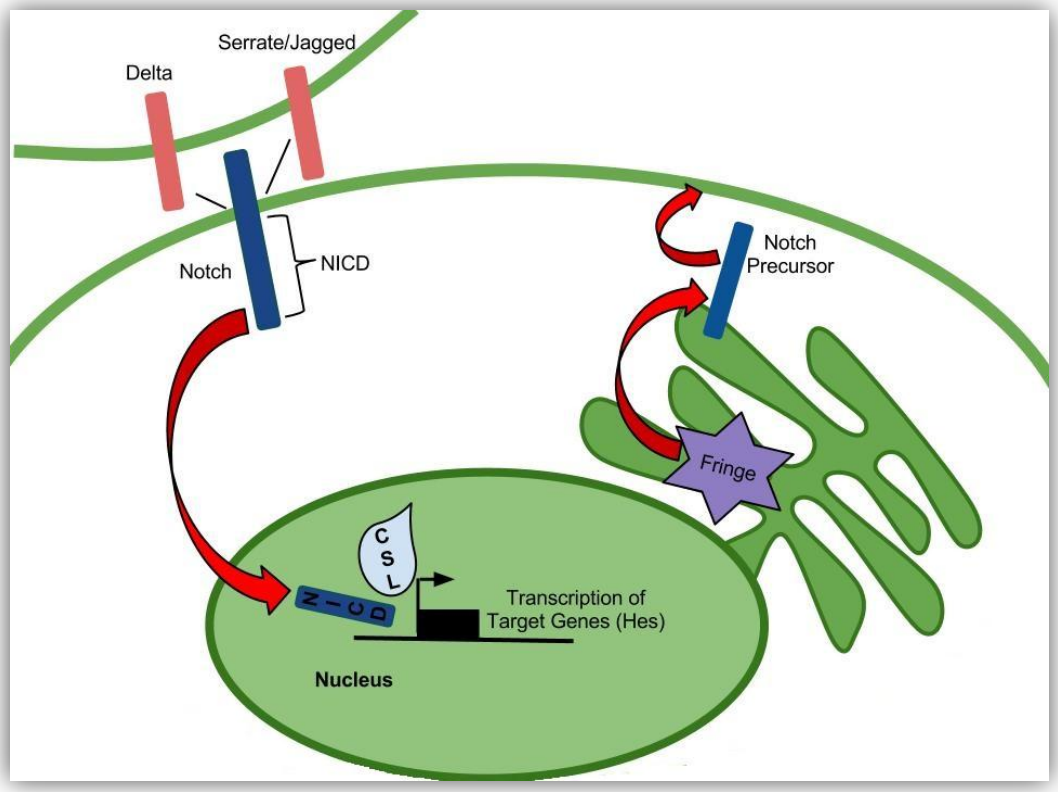

Fig. 3 Notch Signaling. The Notch receptor binds with its ligands, Delta and Serrate/Jagged, triggering release of the NICD. The NICD is then translocated into the nucleus where it acts with its DNA binding partner, CSL, to transcribe its target genes. The Fringe family of glycosyltransferases acts in the Golgi to modify the notch precursor by adding sugars to it and subsequently modifying Notch's affinity for its ligands.

Although Notch signaling controls many aspects of development, the family of Notch proteins is actually quite small. For instance, *Drosophila* has only one Notch receptor gene, *Caenorhabditis elegans* has two, and some vertebrates have four (Table 1) (Weinmaster and Kintner 2003; Haines and Irvine 2003). Multiple tandem-array epidermal growth factor (EGF)-like repeats within the extracellular ligand-binding domain are conserved

between all species' Notch proteins (Weinmaster and Kintner 2003). Although there are only four Notch receptor genes in mammals, they interact with three Delta ligand paralogues and two Jagged gene paralogues (Table 1), which allows for differential signaling between them (Haines and Irvine 2003).

The family of Notch signaling proteins regulates cell fate decisions, specification, and cell differentiation (Lewis 1998). In the most posterior PSM, Notch pulses on and off, while in the most anterior PSM, Notch signaling is fixed in a half-segmental pattern, and then between those two regions, Notch is expressed in a wave that covers a distance of about three somites (Weinmaster and Kintner 2003). This expression pattern is directly related to the outcome of somitogenesis, a segmented and pre-patterned body plan.

Developmental anomalies in humans have been attributed to defects in the Notch pathway and subsequent somite patterning (Hollway and Currie 2005; Sparrow et al. 2005; Loomes et al. 2007; Turnpenny et al. 2007). Segmentation defects of the vertebrae (SDV) encompasses many common defects that occur in humans such as congenital scoliosis, spondylocostal dysostosis (SCD), Alagille syndrome (AGS), and cerebral autosomal dominant arteriopathy with subcortical infarcts and leukoencephalopathy (CADASIL) (Turnpenny et al. 2007). Although many syndromes and disorders include defects of vertebral segmentation, many of their underlying causes are unknown. AGS and CADASIL, although commonly associated with vertebral defects, also cause defects in angiogenesis as well as liver and ocular

problems (Turnpenny et al. 2007). AGS has been correlated to a mutation in *JAG1* and *NOTCH2* while CADASIL has been attributed to a mutation in *NOTCH3* (Turnpenny et al. 2007). SCD, which affects the axial skeleton, has four subtypes attributed to mutations of *DLL3*, *MESP2*, *LFNG*, and *HES7* respectively (Sparrow et al. 2005; Turnpenny et al. 2007; Fisher et al. 2012). In addition to human identified diseases, the mouse model has been used extensively to study the Notch pathway's involvement in vertebrate development. Recently, it was identified in mice that mutations in *Dll3* and *Lfng* alter the pattern of the multifidus, a muscle that extends along the thoracic and lumbar vertebrae (Fisher et al. 2012).

Lunatic Fringe

Members of the Fringe family of glycosyltransferases, including *Lfng*, *Manic fringe* (*Mfng*), and *Radical fringe* (*Rfng*), are able to modify the activity of the Notch receptors by adding extra sugars moieties to the O-linked oligosaccharides on Notch. The addition of sugars alters the specificity of Notch for its ligands (Weinmaster and Kintner 2003). Specifically, *Lfng* encodes an O-fucose-ß1, 3-N-acetylglucosaminyltransferase (ß3GlcNAcT) that attaches to the Notch receptor which gives the receptor differential preference for certain ligands (Serth 2003, Shifley et al. 2008). In *Drosophila*, where the first orthologue was discovered, *fringe* potentiates Delta-Notch interactions while inhibiting Serrate-Notch interactions. In mammals, where there are many more versions of Notch, its ligands, and the fringe proteins, the receptor-ligand relationship is further complicated (Table 1). *Lfng*

inhibits *Notch1's* interaction with *Jag1* and potentiates the interaction with Delta1, similar to what has been describe in *Drosophila* (Haines and Irvine 2003). In contrast, *Lfng* potentiates the interaction of *Notch2* with both *Jag1* and *Dll1* (Haines and Irvine 2003).

Table 1

Components of the Notch Signaling Pathway in *Drosophila* and Mammals

	Drosophila	Mammals
Receptor	*Notch*	*Notch1* *Notch2* *Notch3* *Notch4*
Ligands	*Delta, Serrate*	*Dll1* *Dll3* *Dll4* *Jag1* *Jag2*
CSL	*Su(H)*	*Rbpj*
Fringe Family	*Fringe*	*Lfng* *Mfng* *Rfng*

Analysis of *Lfng* expression patterns in mouse embryos showed that a new somite boundary is formed at the end of each *Lfng* expression wave suggesting that boundary formation is one of the main functions of *Lfng* (Zhang and Gridley 1998; Serth 2003). Mutations in *Lfng* have resulted in

embryos with irregular somites and an overall disruption of their anterior/posterior patterning (Shifley et al. 2008; Zhang and Gridley 1998; Shifley 2009; Dunwoodie 2009).

In *Drosophila, fringe* is involved in the formation of wing margins, eyes, and lungs (Shifley et al. 2008). *Lfng* is expressed in the brain, neural tube, somites, and PSM in mouse (*Mus musculus*) and chick (*Gallus gallus*) (Shifley et al. 2008). In addition to those areas, *Lfng* expression can also be found in the zona limitans intrathalamica, eye, retina, and otic vesicle in the developing chick, as well as the olfactory placode, myotome, inner ear, tongue, skin, teeth, and hair in the developing mouse (Shifley et al. 2008; Stauber et al. 2009). In mutant mouse embryos, axial extension stops at E10.5, suggesting that *Lfng* plays an important role in maintaining axial extension and body axis elongation (Shifley et al. 2008; Stauber et al. 2009). *Lfng* has been shown to affect somite borders and anterior-posterior patterning in mouse and chick (Zhang and Gridley 1998; Barrantes et al. 1999; Fisher et al. 2012).

Study Summary

Fisher and colleagues (2012) analyzed muscles of both *Lfng*$^{/-}$ and *Dll3*$^{/-}$ adult mice and determined that epaxial muscles exhibit abnormalities and deficits that occurred independently of the previously described osteological defects of the ribs and vertebrae (Fisher et al. 2012). Defects of the multifidus muscle involving its point of attachment and symmetry along the anterior-posterior axis. The multifidus muscle is derived from the epaxial myotome, which serves as a driving force behind our analysis of epaxial

musculature in the *Lfng* knockout. In addition to their published multifidus data, they also observed that the iliocostalis muscle exhibited defects in its attachment sites and in some areas was fused or absent (Fisher, personal communication); this fact brings into question the embryonic events that surround formation of epaxial muscles. This study provides a morphometric analysis of mouse embryonic and fetal back musculature with a focus on the longissimus, iliocostalis, and latissimus dorsi muscles to provide embryonic data that is consistent with adult *Lfng*$^{-/-}$ phenotypes. This analysis provides evidence of an embryonic origin of muscular defects associated with Notch and *Lunatic Fringe*.

In our current analysis, we observed embryonic defects specific to the iliocostalis and longissimus muscles *Lfng*-null background. The iliocostalis had an overall decrease in muscle fiber number and hypotrophic when compared with the *Lfng*$^{+/+}$ genotype. The longissimus muscle had a shorter fiber diameter in the younger embryos, but had normal diameter in the older embryos and neonate. There was no significant difference in muscle fiber number or diameter in the latissimus muscle. These results suggest that the iliocostalis and longissimus muscles of the erector spinae are affected by the absence of *Lfng* more than the latissimus, which derives from a different progenitor muscle group. These data provide additional evidence that *Lfng* plays a role in not only vertebral and rib patterning but in epaxial muscle patterning as well. This information may lead to further understanding of congenital myopathies and muscular dystrophies as well as confounding myogenic issues associated with idiopathic scoliosis.

CHAPTER 2

MATERIALS AND METHODS

Mouse Husbandry

In this study we used CD1 outbred mice and B6/129Sv inbred mice carrying a null mutation allele for *Lfng* that was originally described in Evrard et al. (1998). Mice and embryos were genotyped for the mutant *Lfng* allele using a standard PCR approach with primers that differentiate the mutant and wild type allele (Evrard et al. 1998).

All animals were bred and maintained in the vivarium at Arizona State University on a 10/14 light cycle with ad libitum access to food and water. ASU is accredited by AAALAC and all animal procedures were carried out in accordance with AAALAC standards. These studies were carried out in compliance with the ASU institutional animal care and use committee under an approved research protocol.

Collection of Embryos and Neonates

CD1 and Lfng heterozygote ($Lfng^{+/-}$) mice were mated overnight and female mice were checked for copulation plugs each morning; midnight was the proposed time of conception for all embryos. The morning on which a copulation plug was found was considered embryonic day E0.5. Females were euthanized by CO_2 hypoxia at gestational ages E14.5 through E17.5. Embryos were dissected from the pregnant uterus in cold phosphate buffered saline (PBS) and transferred into 4.0% paraformaldehyde (PFA) for fixation overnight.

Histology

CD1, *Lfng* null (Lfng $^{-/-}$), and *Lfng* wild-type (*Lfng*$^{+/+}$) littermate embryos and/or neonates were washed five times in room temperature PBS followed by dehydration with a series of graded ethanol (EtOH) (25%, 50%, and 75%). After dehydration, the specimens were exposed to xylene for 20 minutes with shaking and then fresh xylene for 20 minutes in a warmer. Next, paraffin embedding wax was added to the warm xylene creating a solution of approximately 50% wax, 50% xylene. The embryos or neonates were left in this solution for 1 hour. The wax/xylene mixture was then replaced with 100% wax for 1 hour and fresh 100% wax overnight. .

Transverse sections of embryos and neonates were made using a rotary microtome set at 8μm-10μm. The sections were set on Histobond slides (VWR) and left overnight on a slide warmer. Slides were stained with hematoxylin and eosin (H & E) to increase visibility of cytoplasm (pink) and nuclei (dark blue to black). H & E staining was done by leaving the slides in xylene for 10 minutes to remove the excess wax followed by two washes in 100% EtOH for 3 minutes each. Next, the slides were taken through a series of graded ethanol (95%, 80%, 70%, 50%, 25%) and finally into distilled water (dH_2O) twice for 2 minutes each. The slides were then placed into hematoxylin for 1 minute and then washed in fresh dH_2O until clean. Next, the slides were quickly dipped into acid alcohol (0.04% hydrochloric acid in 95% EtOH) and washed again in fresh dH_2O. Next, the slides were quickly dipped into 1% ammonia (in dH_2O) and washed again in fresh dH_2O. The slides were then taken back through the graded ethanol, stopping at 70%.

Next, the slides were placed into eosin for 1 minute followed by progression to 100% EtOH through 80% EtOH and 95%EtOH. The slides were then left in 100% EtOH for 3 minutes followed by xylene for 6 minutes. The slides were mounted with Permount and standard cover slips and left overnight to dry.

Analysis of Embryos

CD1 and *Lfng*$^{+/+}$ embryos were used to describe the normal range of development for the epaxial muscles and to determine the proper age ranges for the analysis of *Lfng* deficient embryos. Tissue sections were photographed in brightfield at 10x magnification and complied into composite images for muscle identification. Muscles of the cervical, thoracic, and lumbar regions were identified in embryos of ages E15.5 to E17.5. Muscles identified in the cervical region included the biventer/complexus, rhomboids, supraspinatus, infraspinatus, subscapularis, longissimus, and trapezius. In the thoracic region, we identified the trapezius, rhomboids, latissimus dorsi, multifidus, longissimus, iliocostalis, intercostalis, and serratus ventralis. In the lumbar region we identified the latissimus dorsi, longissimus, and multifidus.

In the *Lfng* embryos, we focused our analysis on the thoracic region of the embryo, specifically concentrating on the longissimus, iliocostalis, and latissimus dorsi muscles. Any differences in fiber orientation, attachment point, fiber density, fiber diameter, and overall muscle development were noted. Tissues were photographed in bright-field using a microscope camera in 10x and 40x magnifications and compiled into composite images using Adobe Photoshop or analyzed as single images. Images of individual muscle groups (iliocostalis, longissimus, and latissimus dorsi) were superimposed

under a histology grid to count fiber number and calculate fiber density. The same images were also used to calculate average fiber diameter by using ImageProPlus software with biological measurement capabilities.

Statistical Analysis

A one-tailed *t*-test with the α set at 0.05 was used to determine if there was a statistically significant difference in fiber number and fiber diameter between *Lfng* deficient embryos and their littermates. In addition to the initial *t*-test, a One Way Analysis of Variance (ANOVA) was used to determine if there was any significant difference in the mean fiber number and diameter of the muscles between the two groups. The results of the ANOVA have been compiled into Table 2 and Table 3.

CHAPTER 3

RESULTS AND DATA ANALYSIS

The role of *Lunatic Fringe* in muscle patterning was assessed by first defining the normal range of muscle development using an inbred strain of CD1 mice coupled with classic histological techniques including paraffin imbedding, sectioning, and hematoxylin and eosin staining. Using wild-type embryos from ages E15.5 to neonate, we were able to map muscles of the cervical, thoracic, and lumbar region as they developed from primary muscle masses into muscle groups. During embryonic age E15.5 the transition from primary to secondary muscle masses became clear and was followed by rapid expansion and separation of muscle groups. In the thoracic region the longissimus, iliocostalis, and latissimus dorsi, as well as surrounding muscles were clearly distinguished from one another by E17.5 (Figure 4). This primary atlas of thoracic back musculature was used as a guide for the *Lunatic Fringe* analysis. This atlas also provides a tool for which other defects of trunk musculature can be analyzed.

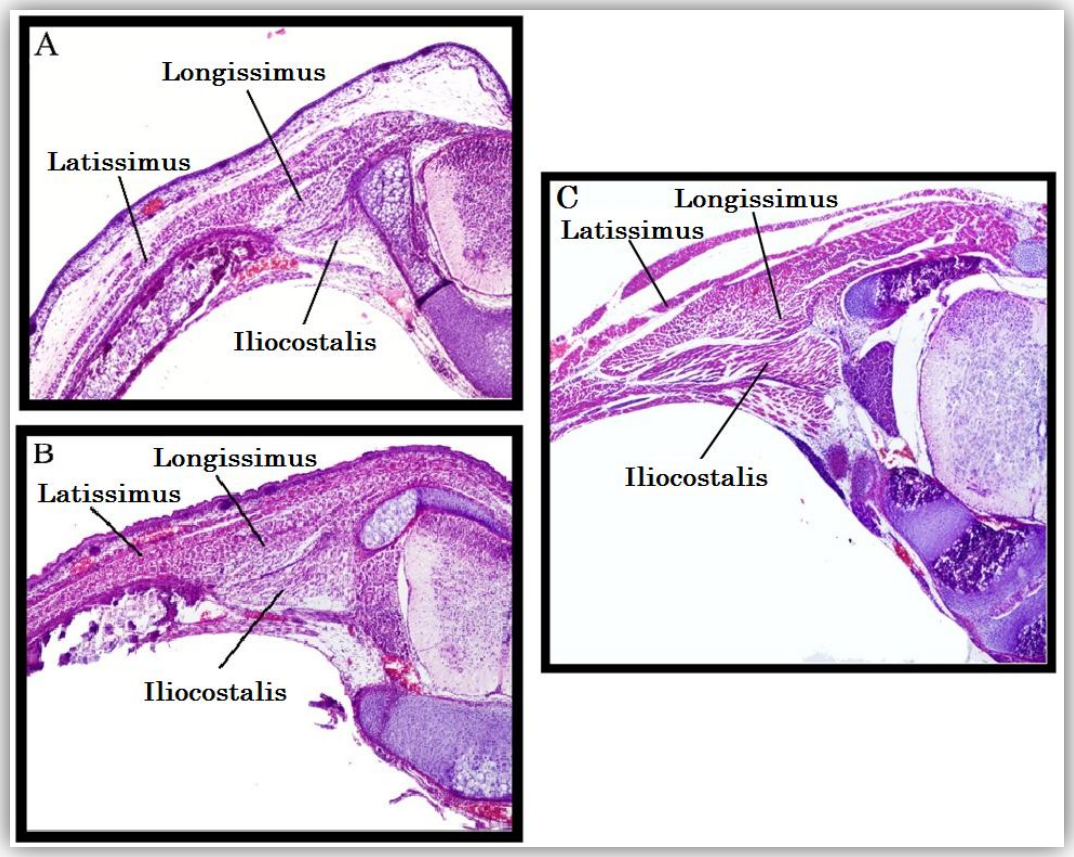

Fig. 4 Morphology of thoracic muscle formation. Embryos were embedded in wax, sectioned, and stained with hematoxylin and eosin. All images are taken at the thoracic level to visualize the latissimus dorsi, longissimus, and iliocostalis muscles. At age E15.5 (A) early muscle masses can be seen. E17.5 (B) embryonic muscle masses continued to develop and become noticeably more distinct. Neonatal (C) muscles are larger, more defined, and more adult-like than the embryonic muscle masses.

Lfng$^{-/-}$ embryos and their wild-type littermates were examined using the same histological techniques mentioned above to explore the effect of *Lunatic fringe* on epaxial muscle patterning and development. E15.5- E17.5 embryos as well as neonates were examined. Neonates were included in this analysis to confirm that the mutation was not post-natal lethal. Fiber density and diameter were measured for longissimus, iliocostalis, and latissimus dorsi muscles in the embryos and neonates. Those muscles were chosen because the longissimus and iliocostalis muscles both derive from the epaxial region of the somite, whereas the latissimus dorsi derives from the hypaxial region. A superimposed histological grid was used to calculate density and ImageProPlus measuring software was used to calculate muscle fiber diameter. After all measurements were established a one-way ANOVA test was used to determine statistical significance between the groups. For both fiber density and fiber diameter, an average of 5 embryos (n=5) was used for each age, genotype, and muscle group. This yielded a total of 39 embryos analyzed ranging from E15.5 to neonate and having a genotype of *Lfng* $^{+/+}$ (n=20) and *Lfng* $^{-/-}$ (n=19).

The iliocostalis muscle in the *Lfng*$^{-/-}$ embryos showed a significant decrease in muscle fiber density across all age groups (P= <0.0001 for embryos; P= <0.0005 for neonates) when compared to the littermates (Figure 5A). Muscle fiber diameter also differed significantly between the two genotypes across most ages (P= <.0005 for E15.5, E17.5, and neonates; P= 0.13 for E16.5) (Figure 5B). In the *Lfng*$^{+/+}$ embryos, muscle fiber density decreased as muscle fiber diameter increased, a trend that was also seen in

the *Lfng*$^{-/-}$ embryos, but to a lesser degree. Staining with H&E further revealed the structure of the iliocostalis muscle, showing a very different morphology (less fibers and less collagen) between the *Lfng*$^{-/-}$ and the *Lfng*$^{+/+}$ specimens (Figure 6).

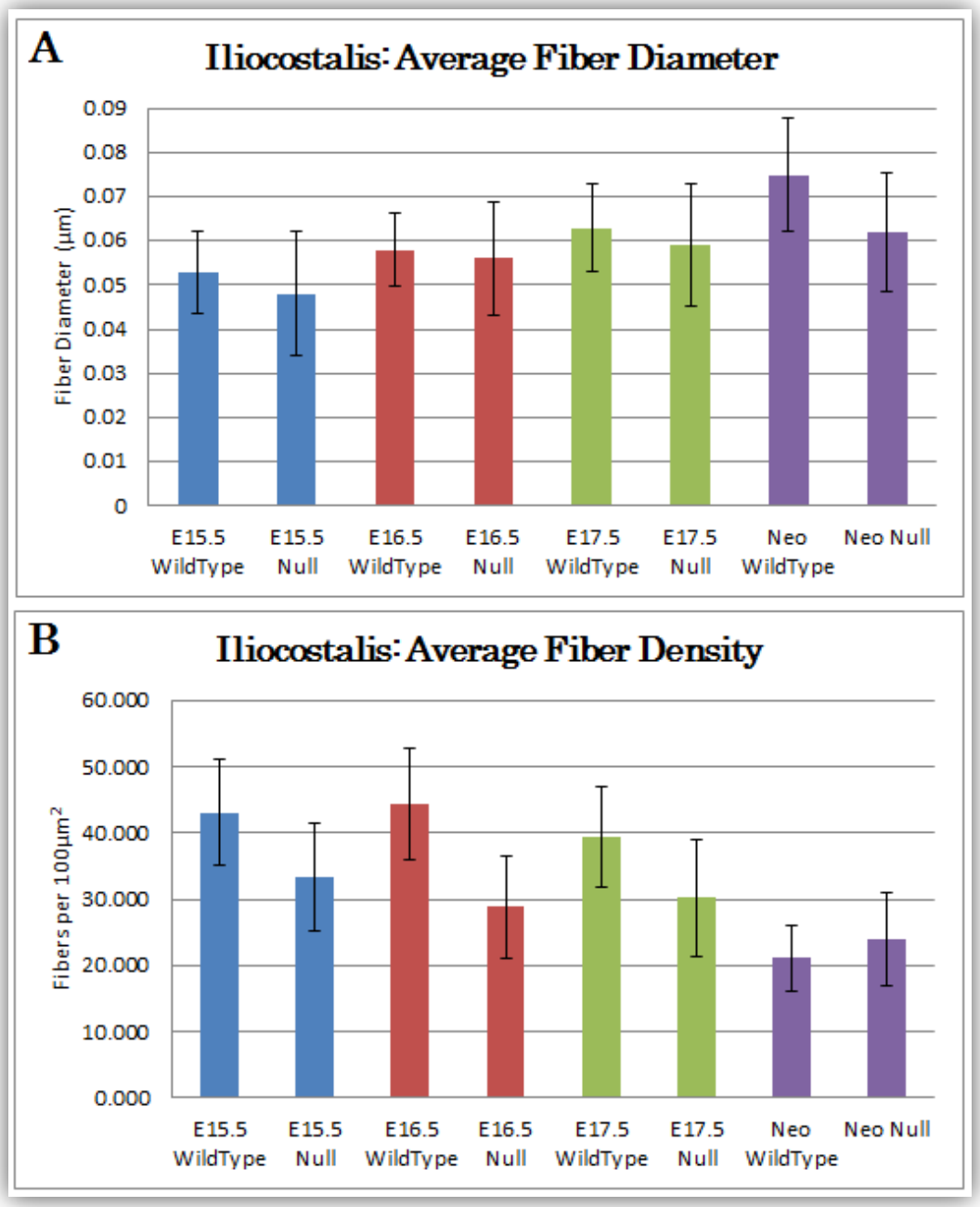

Fig. 5 *Lfng*$^{-/-}$ mice display a defect in formation of the iliocostalis muscle when compared to wild-type littermates. Fiber density (A) in the *Lfng*$^{-/-}$ is less than the wild-type littermates by a statistically significant value (P= <.0005 for all ages). Fiber Diameter (B) in the *Lfng*$^{-/-}$ is less than the wild-type littermates by a statistically significant value (P= <.005 for all ages). In the wild-type littermates, fiber density decreases as fiber diameter increases corresponding to normal growth of the iliocostalis muscle; although this trend is relatively true in the *Lfng*$^{-/-}$ mice, the density and diameter are much less leading to an overall decrease in the iliocostalis muscle.

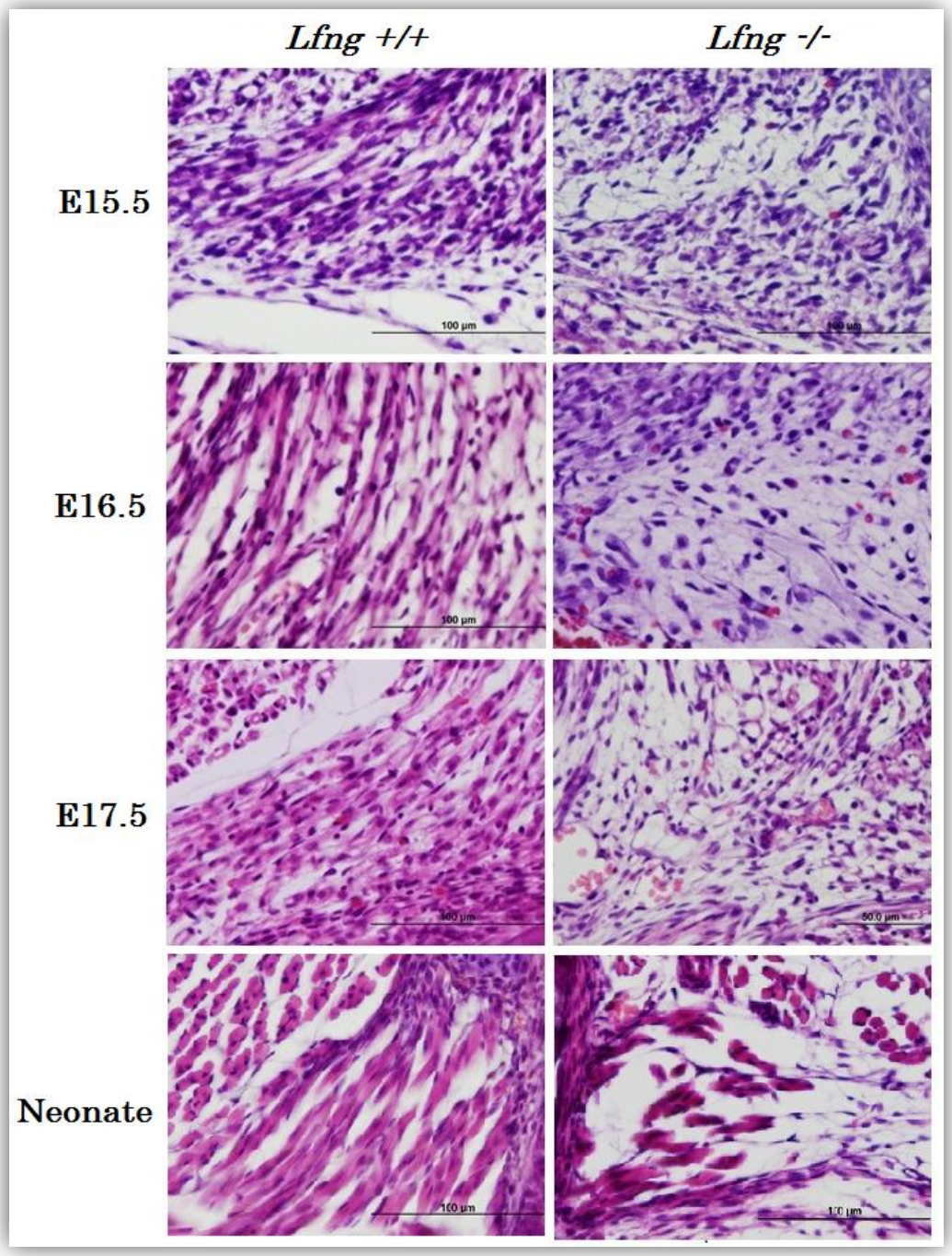

Fig. 6 Morphology of the iliocostalis muscle in *Lfng*$^{-/-}$ and *Lfng*$^{+/+}$ littermates. Tissues were sectioned at 8µm and stained using hematoxylin and eosin. In the *Lfng*$^{-/-}$ specimens the iliocostalis is less dense and the fibers that make up the muscle have a smaller diameter than in the *Lfng*$^{+/+}$.

The longissimus muscle in the *Lfng*$^{-/-}$ showed a significant difference in fiber diameter in only the youngest (E15.5) embryos (Figure 7A). However, fiber density in the *Lfng*$^{-/-}$ *embryos* was not significantly different for the E15.5 embryos, but was significantly different for the E16.5 (P= 0.035), E17.5 (P= <0.0001), and neonates (P= <0.0001) (Figure 7B). Because diameter was affected in the E15.5 embryos it was expected that the density would not be affected as there would be many more fibers in each histological grid. In the E16.5 embryos, the *Lfng*$^{-/-}$ *specimens* had less fiber density (45.4 per 100μm) than the wild-type littermates (48.2 per 100μm); however, in the E17.5 embryos, the *Lfng*$^{-/-}$ *specimens* had a greater fiber density (46.8 per 100μm) than the wild-type littermates (42.2 per 100μm). The resulting trend shows that in the *Lfng*$^{+/+}$ density increases slightly from E15.5 to E16.5, then decreases from E17.5 to birth. In the *Lfng*$^{-/-}$, density plateaued between E15.5 to E17.5 and did not decrease until birth. Overall, the morphological differences of the *Lfng*$^{-/-}$ and *Lfng*$^{+/+}$ longissimus muscles are less distinct when stained with H&E (Figure 8).

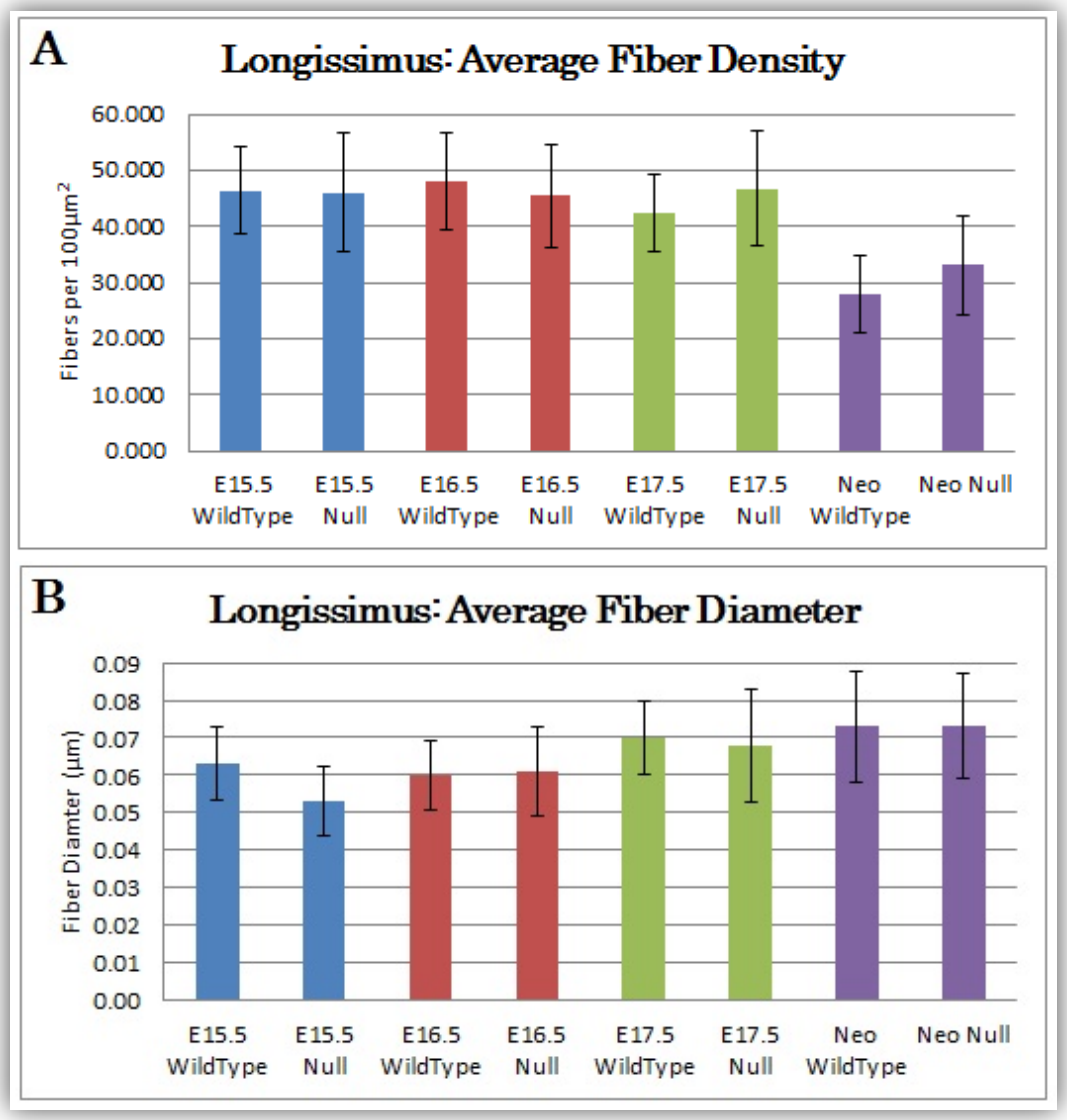

Fig. 7 *Lfng*$^{-/-}$ mice aged E15.5 to neonate display a delay of muscle cell proliferation resulting in decreased density and E15.5 embryos also show a decrease in muscle fiber density that is rescued in the later stages. Fiber density (A) was statistically significant for E16.5, E17.5, and neonatal specimens (P= <.05 for all ages), but was not significant for the youngest group, E15.5. In the older samples (E17.5 and neonates), density is greater in the *Lfng*$^{-/-}$ samples than in the *Lfng*$^{+/+}$ samples. Fiber Diameter (B) was statistically significant in the E15.5 embryos (P=<.0001) but was not significantly significant in the E16.5, E17.5, or neonatal specimens.

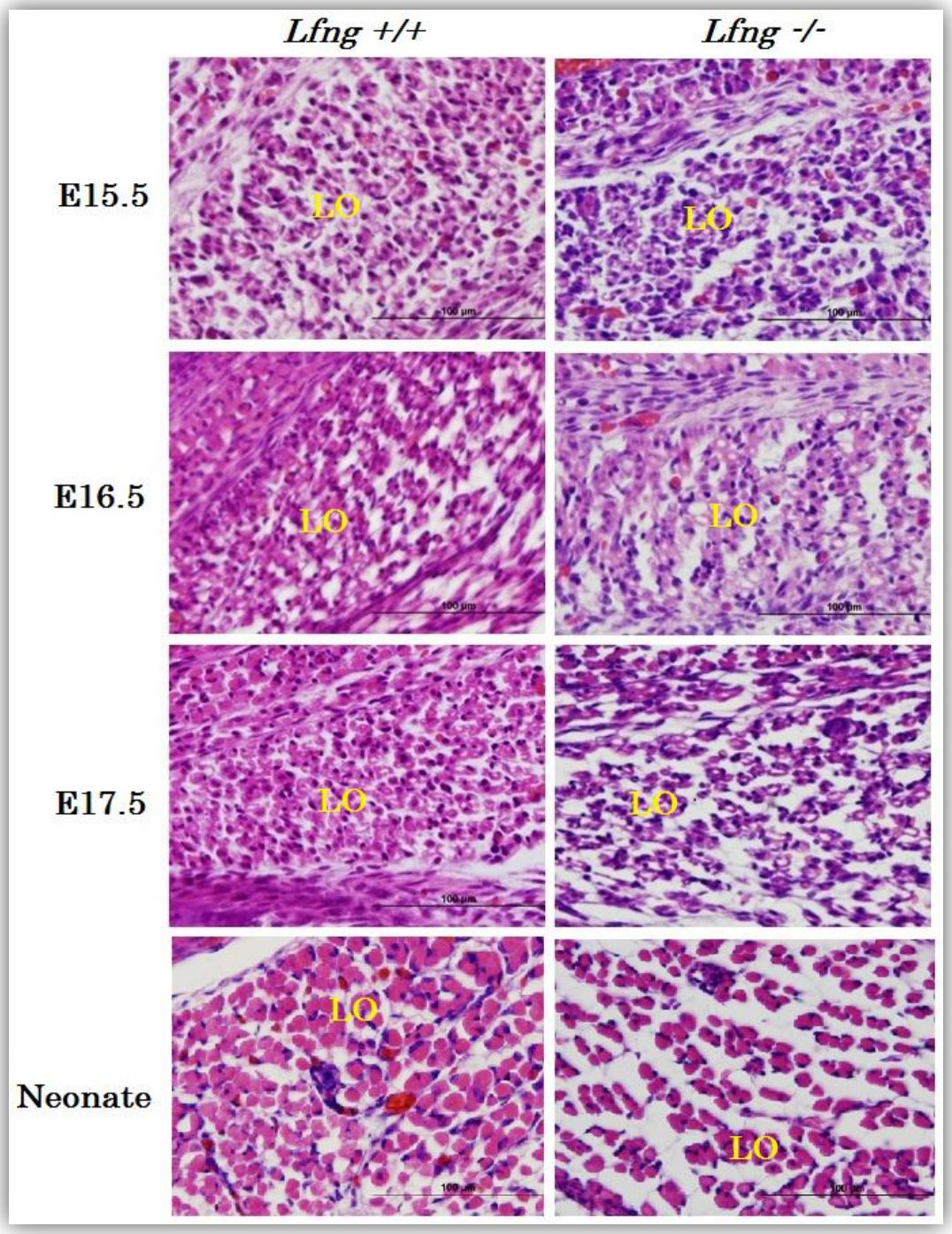

Fig. 8 Morphology of the longissimus muscle in *Lfng*$^{-/-}$ and *Lfng*$^{+/+}$ embryos. Tissues were sectioned at 8μm and stained using hematoxylin and eosin. *Lfng*$^{-/-}$ longissimus muscles are less dense in the E16.5 through neonatal specimens. Lo= Longissimus

The density and diameter of muscle fibers was also examine for the hypaxially-derived latissimus dorsi muscle. This muscle group is superficial and lateral to the longissimus and acts to extend and adduct the arm. The latissimus dorsi muscle was stained with H&E to reveal the similar morphology between *Lfng*$^{-/-}$ and *Lfng*$^{+/+}$ specimens (Figure 10). No significant difference in fiber diameter or density was present when compared to the wild-type littermates (P= >0.2 for all samples) (Figure 9A and 9B).Statistical information for fiber density and fiber diameter for all muscle groups has been compiled into Table 2 and Table 3.

Variations have been reported for the severity of the skeletal defects observed in the *Lfng*$^{+/-}$. Similar morphological variability in the density and diameter could lead to a dampening in morphological differences when averaged. Therefore, the average values of fiber density were graphed with the range of values included (Figure 11). In general, the *Lfng*$^{+/-}$ groups showed a greater range of defects than the *Lfng*$^{+/+}$ groups in the iliocostalis (Figure 11A) and the longissimus (Figure 11B). The latissimus dorsi muscle did not show any substantial difference in range between the two groups (Figure 11C). To further examine the differences seen between individuals, we individually graphed fiber density (Figure 12) and fiber diameter (Figure 13) for each individual of each age and muscle group. It is clear that within each group of the *Lfng*$^{-/-}$ specimens there are individuals that closely resemble the *Lfng*$^{+/+}$ group and individuals with varying degrees of the defects. This analysis offers some insight into the penetrance of the *Lfng* defect as some mutant embryos are affected more than others.

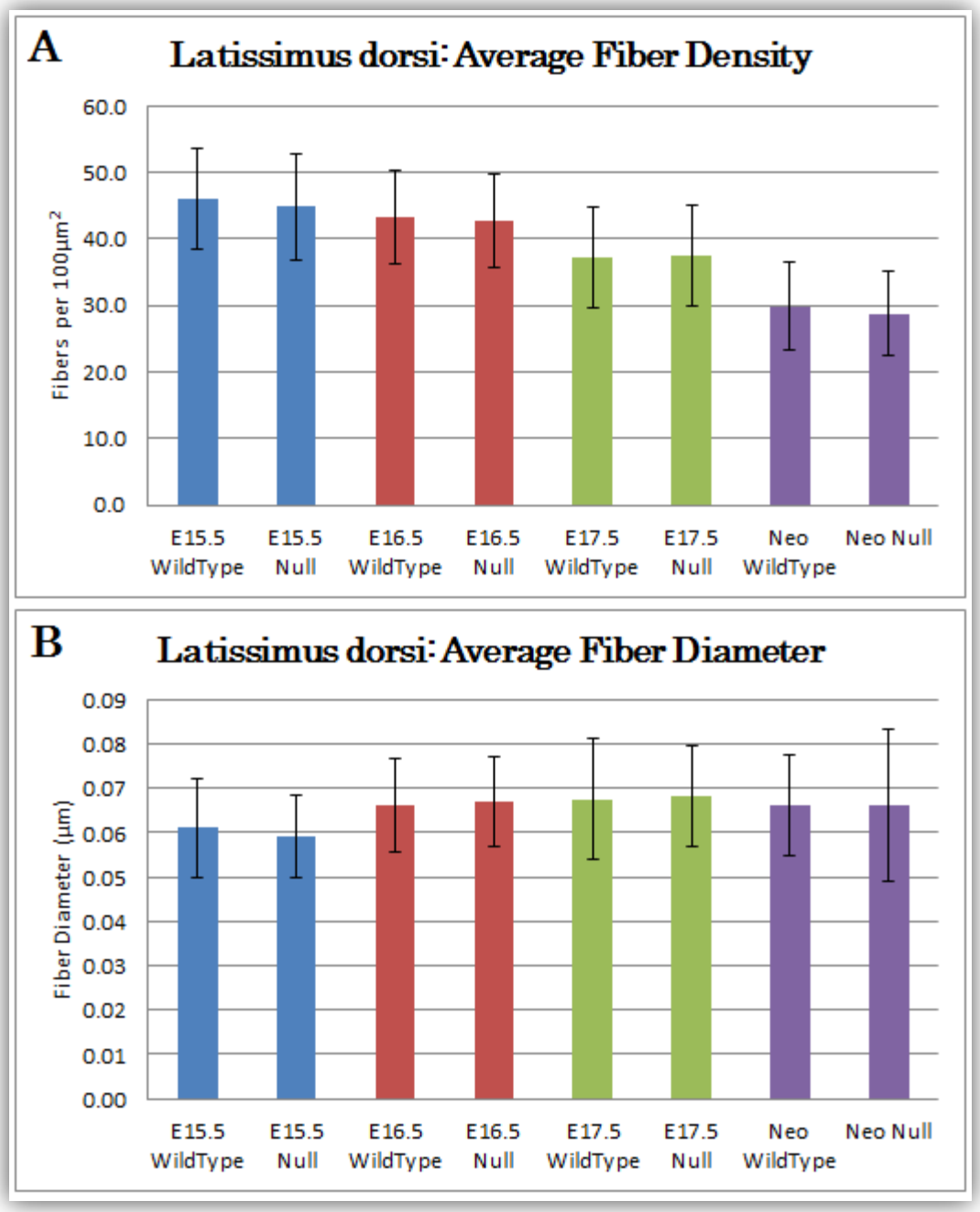

Fig. 9 The development of the latissimus dorsi muscle is not hindered by the *Lfng* knockout. Fiber density (A) in the *Lfng*$^{-/-}$ embryos and neonates (Neo) is not statistically different from the *Lfng*$^{+/+}$ littermates (P= >0.2 for all ages). Fiber Diameter (B) in the *Lfng*$^{-/-}$ embryos and neonates is also not statistically different than the wild-type littermates (P= >0.3 for all ages).

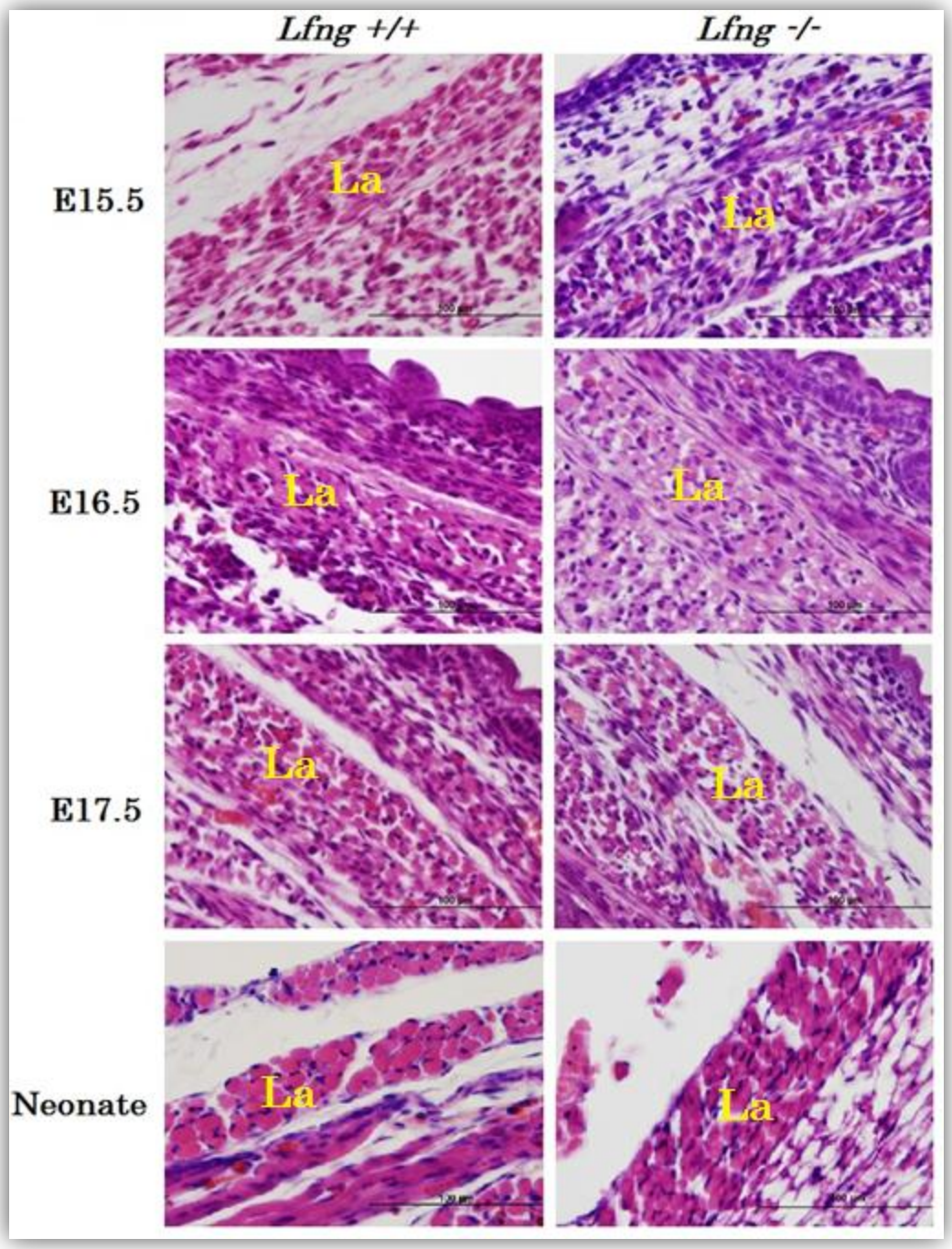

Fig. 10 Morphology of the latissimus dorsi muscle in *Lfng*$^{-/-}$ and *Lfng*$^{+/+}$ littermates. Tissue sections were sectioned at 8μm and stained with hematoxylin and eosin. The latissimus dorsi muscle displays no difference is muscle fiber density or diameter between the two genotypes. La= Latissimus dosri

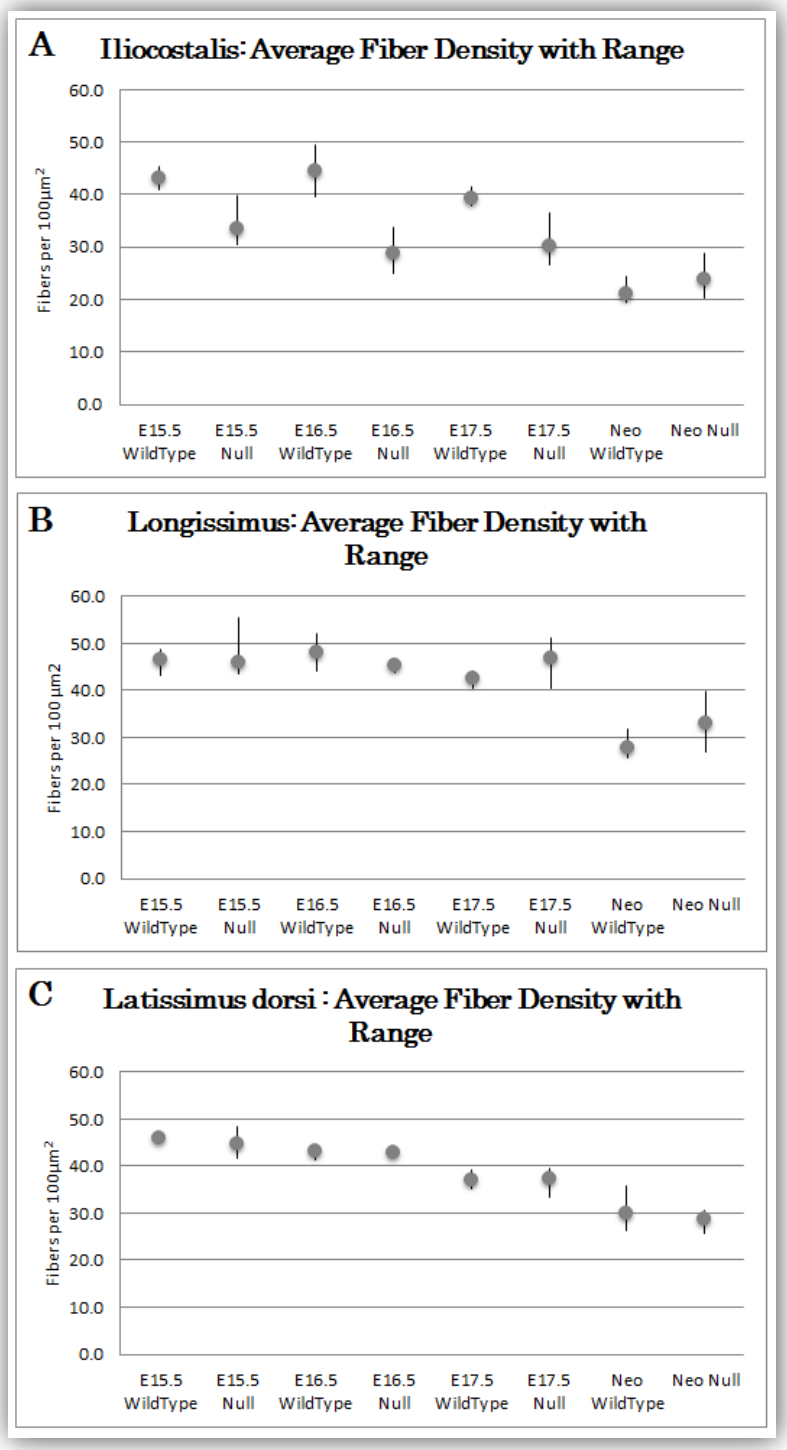

Fig. 11 Average fiber density and range for iliocostalis, longissimus, and latissimus dorsi muscles. In general, the Lfng -/- embryos and neonates show more variation than the *Lfng*$^{+/+}$ embryos in their muscle fiber density in both

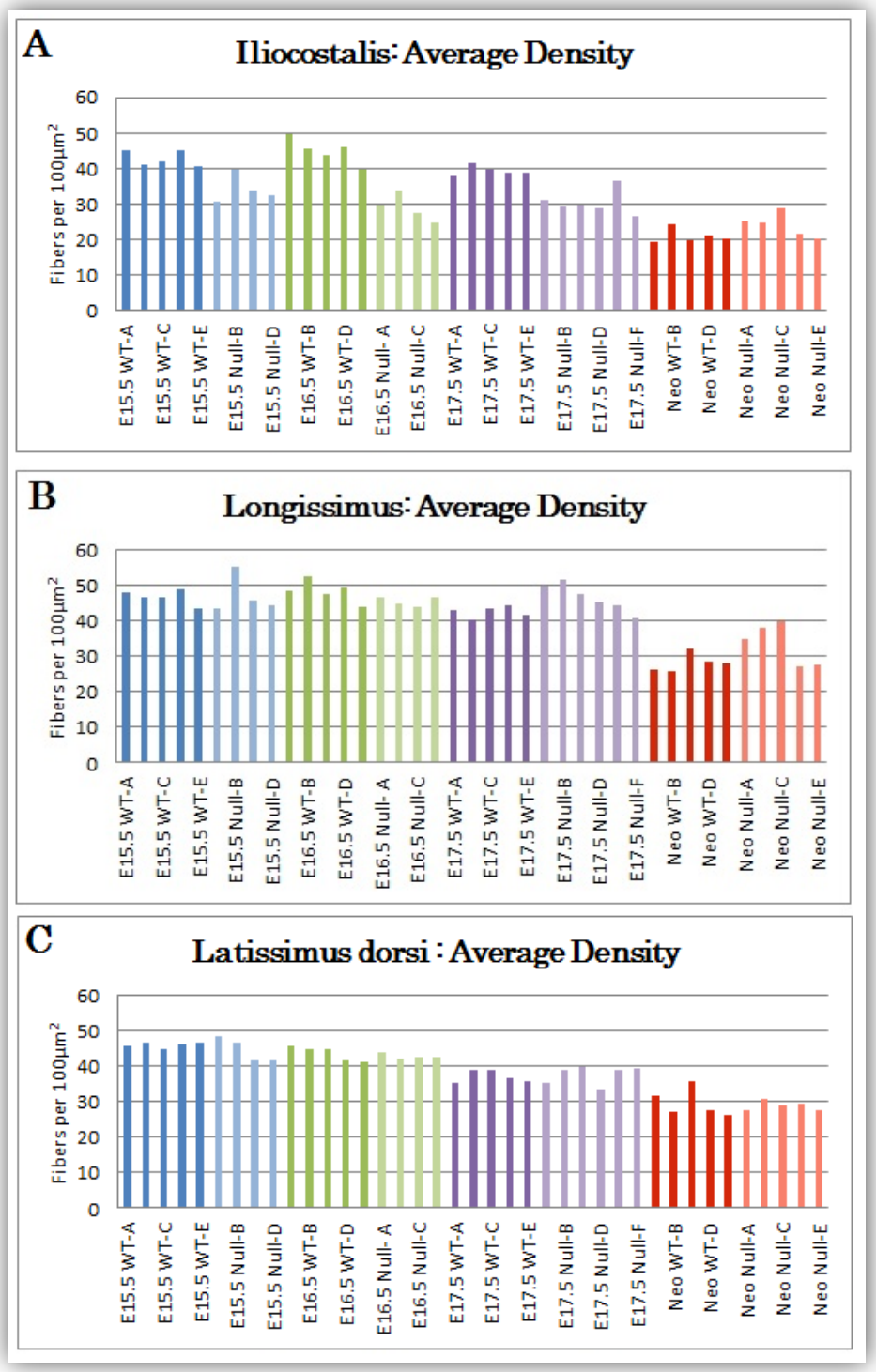

the iliocostalis (A) and longissimus (B) muscles; the latissimus dorsi (C) muscle shows no substantial difference between the two genotypes.

Fig. 12 Individual fiber density for each age, genotype, and muscle group. The iliocostalis (A) and longissimus (B) groups show greater variation within the

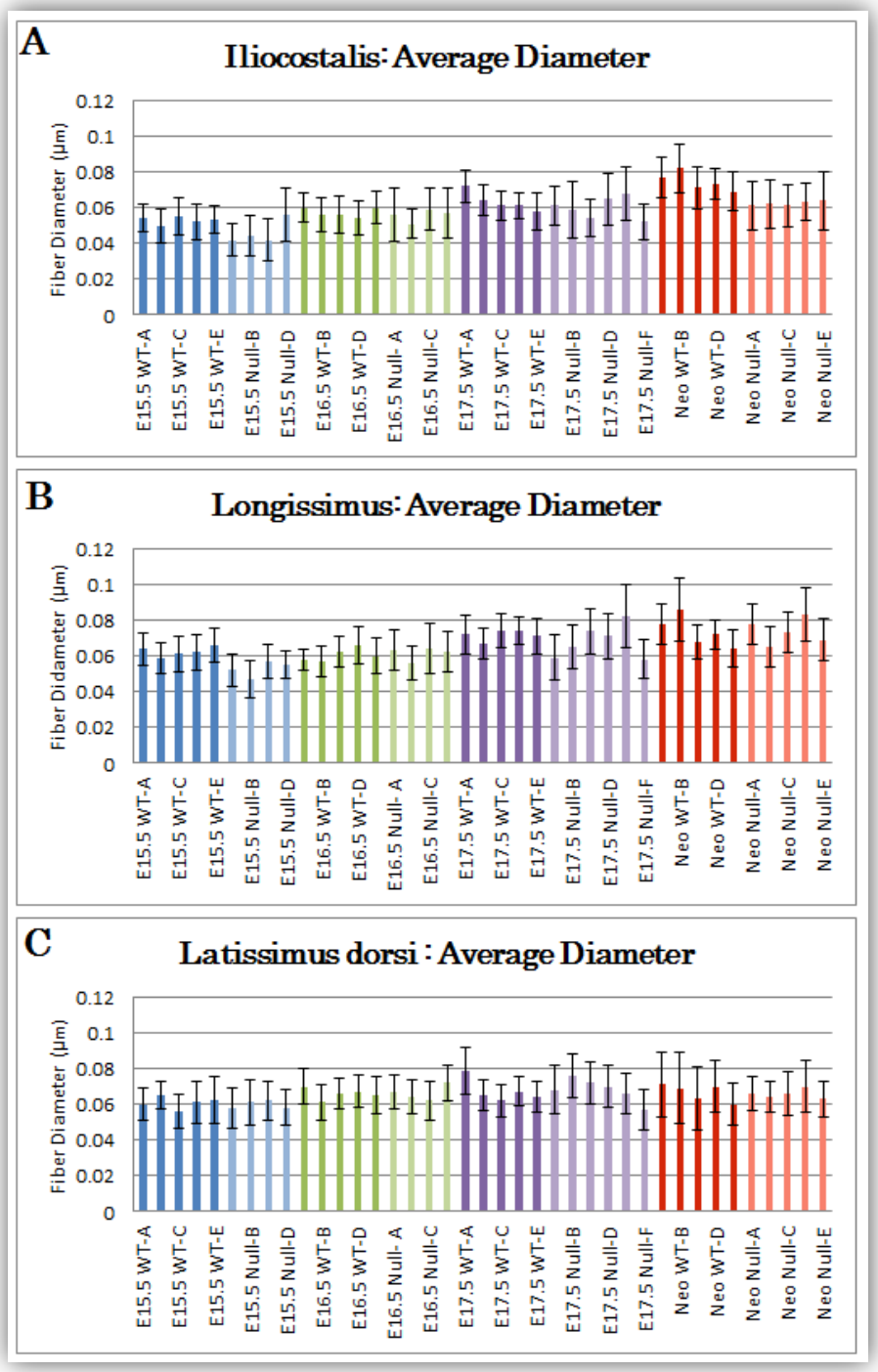

Lfng$^{-/-}$ groups than is seen in the latissimus dorsi (C) group. Error bars were negligible.

Fig. 13 Individual fiber diameter for each age, genotype, and muscle group. Graphing each individual separately, revealed variation within every individual, genotype, and muscle group. The iliocostalis (A) and longissimus

(B) muscle groups contain individuals who are more affected by the knockout than others while in the latissimus dorsi genotype does not have an effect on variation (C).
Table 2

Fiber Density Statistical Analysis for Iliocostalis, Longissimus, and

Latissimus dorsi Muscles

Iliocostalis				
Age	**Genotype**	**N (embryos)**	**Average**	**P**
E15.5	*Lfng*$^{-/-}$	4	33.39	<.0001
E15.5	*Lfng*$^{+/+}$	5	43.07	
E16.5	*Lfng*$^{-/-}$	4	28.80	<.0001
E16.5	*Lfng*$^{+/+}$	5	44.42	
E17.5	*Lfng*$^{-/-}$	6	30.18	<.0001
E17.5	*Lfng*$^{+/+}$	5	39.37	
Neo	*Lfng*$^{-/-}$	5	23.95	0.000464
Neo	*Lfng*$^{+/+}$	5	21.06	
Longissimus				
Age	**Genotype**	**N (embryos)**	**Average**	**P**
E15.5	*Lfng*$^{-/-}$	4	46.08	0.806847
E15.5	*Lfng*$^{+/+}$	5	46.45	
E16.5	*Lfng*$^{-/-}$	4	45.44	0.035407
E16.5	*Lfng*$^{+/+}$	5	48.16	
E17.5	*Lfng*$^{-/-}$	6	46.77	<.0001
E17.5	*Lfng*$^{+/+}$	5	42.42	
Neo	*Lfng*$^{-/-}$	5	33.09	<.0001
Neo	*Lfng*$^{+/+}$	5	27.95	
Latissimus dorsi				
Age	**Genotype**	**N (embryos)**	**Average**	**P**
E15.5	*Lfng*$^{-/-}$	4	44.87	0.284792
E15.5	*Lfng*$^{+/+}$	5	46.03	
E16.5	*Lfng*$^{-/-}$	4	42.76	0.632059
E16.5	*Lfng*$^{+/+}$	5	43.23	
E17.5	*Lfng*$^{-/-}$	6	37.48	0.708591
E17.5	*Lfng*$^{+/+}$	5	37.13	
Neo	*Lfng*$^{-/-}$	5	28.8	0.205786
Neo	*Lfng*$^{+/+}$	5	29.88	

Table 3

Fiber Diameter Statistical Analysis for Iliocostalis, Longissimus, and Latissimus dorsi Muscles

Iliocostalis				
Age	**Genotype**	**N (embryos)**	**Average**	**P**
E15.5	*Lfng*$^{-/-}$	4	0.048	0.000405
E15.5	*Lfng*$^{+/+}$	5	0.053	
E16.5	*Lfng*$^{-/-}$	4	0.056	0.125391
E16.5	*Lfng*$^{+/+}$	5	0.058	
E17.5	*Lfng*$^{-/-}$	6	0.059	0.000199
E17.5	*Lfng*$^{+/+}$	5	0.063	
Neo	*Lfng*$^{-/-}$	5	0.062	<.0001
Neo	*Lfng*$^{+/+}$	5	0.075	
Longissimus				
Age	**Genotype**	**N (embryos)**	**Average**	**P**
E15.5	*Lfng*$^{-/-}$	4	0.053	<.0001
E15.5	*Lfng*$^{+/+}$	5	0.063	
E16.5	*Lfng*$^{-/-}$	4	0.061	0.198391
E16.5	*Lfng*$^{+/+}$	5	0.060	
E17.5	*Lfng*$^{-/-}$	6	0.068	0.061942
E17.5	*Lfng*$^{+/+}$	5	0.070	
Neo	*Lfng*$^{-/-}$	5	0.073	1
Neo	*Lfng*$^{+/+}$	5	0.073	
Latissimus dorsi				
Age	**Genotype**	**N (embryos)**	**Average**	**P**
E15.5	*Lfng*$^{-/-}$	4	0.059	0.2993
E15.5	*Lfng*$^{+/+}$	5	0.061	
E16.5	*Lfng*$^{-/-}$	4	0.067	0.320347
E16.5	*Lfng*$^{+/+}$	5	0.066	
E17.5	*Lfng*$^{-/-}$	6	0.068	0.424078
E17.5	*Lfng*$^{+/+}$	5	0.068	
Neo	*Lfng*$^{-/-}$	5	0.066	0.920388
Neo	*Lfng*$^{+/+}$	5	0.066	

CHAPTER 4

DISCUSSION

Successful development of the vertebrate body plan requires segmentation and acquisition of positional information along the anterior/posterior axis. It is now clear that the Notch signaling pathway is intimately related to the molecular events regulating these processes. Here I have presented evidence for a previously undescribed role for the Notch modifier, Lfng, regulating the maturation of discrete muscle groups during fetal development. The following paragraphs will briefly revisit the importance of *Lfng* while also describing our results and offering several explanations for the defects seen in the *Lfng*$^{-/-}$ embryos. Among these explanations are defects in proliferation, differentiation, maturation, and events of myogenesis. A description of adult *Lfng*$^{-/-}$ mice dissections, done by Fisher et al. (2011), will offer supporting evidence for this analysis. I will then present implications of this research on studying diseases such as spondylocostal dysostosis and scoliosis. Following that, I will also discuss potential defects of neurogenesis in *Lfng*$^{-/-}$ animals, how that relates to our results, and offer a model that may explain our results. Lastly, I will introduce future directions for this research that will aid in further classifying the mechanisms of Notch signaling.

Many Notch signaling pathway mutants do not survive postnatally due to developmental defects in the respiratory and circulatory systems. However, there are live births among the *Lfng*-nulls, which has allowed us to assess adult and prenatal muscle function and form. We chose to focus our

analysis on Epaxial-derived muscles of the deep back because of their location along the anterior/posterior axis and their non-migratory characteristics. Two epaxial muscles, the longissimus and iliocostalis were morphometrically analyzed as well as one hypaxial muscle, the latissimus dorsi. Muscle sections were photographed, and fiber density (hyperplasia) and diameter (hypertrophy) were determined by using a histological grid and measurement software, respectively. Fiber density within a muscle group provides insight on muscle cell proliferation and differentiation, a process referred to as hyperplasia. Muscle fiber diameter, or hypertrophy, provides information on muscle fiber fusion during myogenesis and the protein content (actin and myosin) of a developing muscle cell.

Lfng$^{-/-}$ adult and postnatal mice display defects in bony structures that are intimately related to the regulation of the musculoskeletal patterning. Those defects include fused vertebrae, caudal agenesis, and a shorter and more compact rib cage. The vertebrae and ribs represent the main attachment points for many of the deep back muscles and therefore differences seen in fiber direction, orientation, or general location could be due to defects in attachment points. Fiber diameter and density, however, should not be affected by bony attachments when other morphological features may be changed. This fact is the main reason a morphometric approach was used for this analysis.

The iliocostalis muscle showed significant differences in both hyperplasia and hypertrophy and morphological differences were clearly seen in histological sections. The iliocostalis muscle in both the *Lfng*$^{-/-}$ and *Lfng*$^{+/+}$

groups displayed a trend in which the density of the muscle decreased as the diameter increased, however in the *Lfng*$^{-/-}$ *embryos* this trend was present to a much lesser degree.

Fiber diameter of the longissimus was only significantly different in the E15.5 embryos. Fiber density was significantly different in the E16.5 and E17.5 embryos as well as the neonates, but was not significantly different in the E15.5 embryos. The *Lfng*$^{-/-}$ specimens started developing with approximately the same or less fiber density than the wild-type littermates, but as they continued to develop the *Lfng*$^{-/-}$ *embryos* had greater fiber density than their wild-type littermates. This is because the *Lfng*$^{+/+}$ longissimus muscle fibers were increasing in size at a stable rate that was relative to the overall size of the muscle. The *Lfng*$^{-/-}$ longissimus muscle fibers were also increasing in size, but not relative to the overall size of the muscle, resulting in a less dense muscle.

The average fiber density with the range of values was graphed for each muscle group, age, and genotype, revealing that the iliocostalis and longissimus muscles in the *Lfng*$^{-/-}$ embryos showed greater variation than the *Lfng*$^{+/+}$ specimens. This finding corresponds with other research involving *Lfng*$^{-/-}$ mice and muscular defects (Fisher et al. 2012). To further confirm this, each individual's fiber density was analyzed separately for muscle group and age. It was confirmed that the iliocostalis and longissimus showed a range of average densities within the group of *Lfng*$^{-/-}$ embryos, and that some individuals were affected more than others within the same age. Within each individual the standard deviation for fiber density was negligible.

Fiber diameter was also analyzed separately for each individual, age, and muscle group; however, in this analysis the standard deviation within each group was large enough to reveal that within each individual there is a variety of fiber diameters that comprise each muscle. Between the ages of E15.5 to birth the muscles are rapidly undergoing secondary myogenesis and fiber maturation, so having variation in fiber diameter within an individual is expected. A few individuals did have iliocostalis and longissimus muscles fiber diameters that were more affected than others within the same group, but this difference was not as severe as the difference in fiber density.

The latissimus dorsi muscle showed no significant difference in hyperplasia or hypertrophy between the *Lunatic fringe* null and wild-type littermates. Because the latissimus dorsi muscle is derived from the hypaxial region of the myotome this raises the possibility that hypaxial derived muscles are not as dependent on *Lfng* activity during development. The results of this analysis suggest that the epaxial muscles, but not the hypaxial muscles, are affected in *Lunatic fringe* null mice. The extent of the defects seen, however, varies between specific muscle groups and time points in development. In the case of the iliocostalis, it is clear that the *Lfng*$^{-/-}$ embryos' muscles on average had a decrease in muscle hyperplasia and hypertrophy. This defect represents a developmental deficiency in muscle fiber proliferation, differentiation, and maturation, due to the consequences of constitutively active Notch. Additionally, this data shows that although the iliocostalis is attached to the ribs, which are severely affected in the *Lfng*$^{-/-}$, the muscle group is dependently affected by the *Lunatic fringe* knockout. In

the case of the longissimus, there did not appear to be a significant defect of hypertrophy, but there was a difference in hyperplasia. The muscle fibers of the longissimus continued to increase in size in both the *Lfng*$^{-/-}$ and the *Lfng*$^{+/+}$, but the *Lfng*$^{-/-}$ did not have as many fibers throughout the muscle. These data suggest that the longissimus muscle, although not as affected as the iliocostalis, has a developmental defect in muscle fiber proliferation.

As previously mentioned, mutations in the human *LFNG* gene have been identified in cases of the vertebral disorder spondylocostal dysostosis (SCD) type 3. SCD is mainly characterized by vertebral and rib anomalies. Because the mouse model is typically used to study human diseases, this data provides additional information on SCD and its range of defects. Many other vertebral defects in humans including idiopathic scoliosis are accompanied by both primary and secondary muscular defects. A paradigm shift in which musculature is analyzed in addition to the obvious bony defects of vertebral disorders is essential in understanding the full range problems that can arise during segmentation and the mechanisms that encompass those disorders.

In a mutant such as *Lfng*$^{-/-}$, defects in neurogenesis may be expected; the extent of those defects however, has not been classified. Studies of neurodevelopment as it relates to timing of muscle development have had conflicting results depending on the type of muscle development (epaxial vs. hypaxial) and the organism; however, it is clear that Notch is essential for differentiation of nerve cells during development, and nerves are critical for secondary myogenesis. A mouse model lacking *Lfng*, a key regulator of Notch, would be unable to undergo proper gene transcription and be unable to guide

proper differentiation. If nerve precursor cells receive mixed signals from Notch, they may be unable to differentiate and therefore unable to direct secondary myogenesis. Additionally, because Lfng$^{-/-}$ embryos only display defects in the epaxial musculature, this neurogenic defect would have to be specific to the dorsal ramus of the spinal nerves as they are the source for innervation of epaxial muscles.

The novel data provided by this morphometric study has brought to light new information regarding the development of epaxial musculature in the *Lfng*$^{-/-}$ and *Lfng*$^{+/+}$ mouse. Fiber density and diameter are important in the consistent development, function, and rigidity of muscle groups and the defects presented here represent the effect of *Lfng* on their development. Defective genes involved in the Notch signaling pathway, such as *Lfng*, often display observable defects of the skeletal system, but as shown here, they also display defects of the muscular system. This further confirms the importance of Notch signaling in somitogenesis, boundary formation, and musculoskeletal patterning, and opens the door for new questions concerning Notch's role in myogenesis.

During myogenesis, Notch signals for proliferation of myogenic progenitor cells. Notch also activates the *Hes* genes, which are involved in several aspects of development. *Hes* genes inhibit *MyoD* which leads to a decrease in differentiation of myoblasts. Notch itself will also inhibit *Myogenin* further decreasing myoblast differentiation. The *Hes* genes will also inhibit the neuronal factors *Ngn2* and *Mash1* which normally activate *Dll1* and *Jagged1* and lead to neurogenesis via lateral inhibition of Notch.

Lfng modifies the Notch receptor, giving it preference for either Delta or Jagged/Serrate. The correct functioning of this complex interaction is necessary for correct Notch signaling and subsequent developmental events (Figure 14). In *Lfng* deficient mice, this interaction is severely disrupted, leading to a decrease in muscle hyperplasia and hypertrophy in the epaxial muscles.

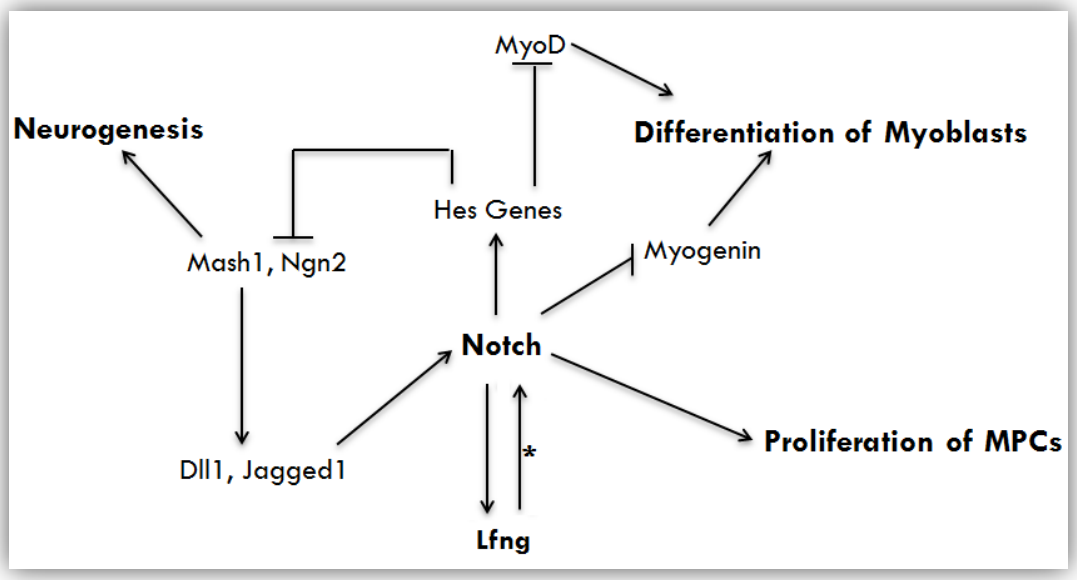

Fig. 14 The role of Notch in myogenesis. Notch signaling inhibits differentiation of myoblasts, activates proliferation of myogenic progenitor cells, and is involved in lateral inhibition during neurogenesis. Lfng is activated by Notch and in return modifies the Notch protein. (*Modifier)

In the future, it will be necessary to further determine the role of innervation in directing formation of the iliocostalis and longissimus muscles. That data would aid in classifying the complex defects associated with *Lfng*

and the Notch signaling pathway. Additionally, other muscle groups that are derived from both epaxial and hypaxial myotome should be morphometrically analyzed and compared to our data and the data in Fisher et al. (2012). The deficiencies of the iliocostalis and longissimus are primary defects of the developing myotomal region in the somite. With that in mind, tracing of muscle cell lineages at earlier ages such as E10.5 to E15.5 could shed light on the origin of the epaxial defect in the *Lfng*$^{-/-}$ embryos.

The impetus behind this morphological study is to further understand the mechanism of Fringe modified Notch signaling as it relates to embryonic cell patterning and muscle development. We know that LFNG protein modulates the Notch receptor pathway, but there have been suggestions that *Lfng* may also work by associating with Notch, or that *Lfng* itself may have alternative functions such as cell signaling (Wu et al. 1996; Ju et al. 2000). Future experiments should also consist of determining the exact mechanism of interaction between all of the Notch proteins (NOTCH1, NOTCH2, NOTCH3, and NOTCH4), their ligands (DLL1, DLL3, DLL4, JAG1, and JAG2), and the different fringe proteins (LFNG, MFNG, and RFNG) within the cell (Haines and Irvine 2003). Understanding the full range of roles for the Fringe family of proteins will offer additional information about early embryonic musculoskeletal patterning, boundary formation, and defects associated with signaling cascades.

REFERENCES

Alvares, L.E., F.R. Schubert, C. Thorpe, R.C. Mootoosamy, L. Cheng, G. Parkyn, A. Lumsden, and S. Dietrich. 2003. "Intrinsic, Hox-dependent Cues Determine the Fate of Skeletal Muscle Precursors." *Developmental Cell* 5 (3): 379–390.

Arber, S., S.J. Burden, and A.J. Harris. 2002. "Patterning of Skeletal Muscle." *Current Opinion in Neurobiology* 12 (1): 100–103.

Aulehla, A. 2004. "Segmentation in Vertebrates: Clock and Gradient Finally Joined." *Genes & Development* 18 (17) (September 1): 2060–2067. doi:10.1101/gad.1217404.

Bajanca, Fernanda, Marta Luz, Marilyn J. Duxson, and Solveig Thorsteinsdottir. 2004. "Integrins in the Mouse Myotome: Developmental Changes and Differences Between the Epaxial and Hypaxial Lineage." *Developmental Dynamics* 231 (2) (October): 402–415. doi:10.1002/dvdy.20136.

Barrantes, I.B., A.J. Elia, K. Wünsch, M.H. De Angelis, T.W. Mak, J. Rossant, R.A. Conlon, A. Gossler, and J.L. de la Pompa. 1999. "Interaction Between Notch Signalling and Lunatic Fringe During Somite Boundary Formation in the Mouse." *Current Biology* 9 (9): 470–480.

Bismuth, K., and F. Relaix. 2010. "Genetic Regulation of Skeletal Muscle Development." *Experimental Cell Research* 316 (18): 3081–3086.

Buchberger, A., K. Ragge, and H.H. Arnold. 1994. "The Myogenin Gene Is Activated During Myocyte Differentiation by Pre-existing, Not Newly Synthesized Transcription Factor MEF-2." *Journal of Biological Chemistry* 269 (25): 17289.

Buckingham, M. 2001. "Skeletal Muscle Formation in Vertebrates." *Current Opinion in Genetics & Development* 11 (4): 440–448.

Buckingham, Margaret. 2006. "Myogenic Progenitor Cells and Skeletal Myogenesis in Vertebrates." *Current Opinion in Genetics & Development* 16 (5) (October): 525–532. doi:10.1016/j.gde.2006.08.008.

Burgess, Rob, Alan Rawls, Doris Brown, Allan Bradley, and Eric Olson. 1996. "Requirement of the Paraxis Gene for Somite Formation and Musculoskeletal Patterning." *Nature* 384: 570–573.

Burke, A.C., and J.L. Nowicki. 2001. "Hox Genes and Axial Specification in Vertebrates." *American Zoologist* 41 (3): 687–697.

Carapuco, M. 2005. “Hox Genes Specify Vertebral Types in the Presomitic Mesoderm.” *Genes & Development* 19 (18) (September 15): 2116–2121. doi:10.1101/gad.338705.

Casares, F., M. Calleja, and E. Sanchez-Herrero. 1996. “Functional Similarity in Appendage Specification by the Ultrabithorax and abdominal-A Drosophila HOX Genes.” *The EMBO Journal* 15 (15): 3934.

Christ, B., H.J. Jacob, and M. Jacob. 1977. “Experimental Analysis of the Origin of the Wing Musculature in Avian Embryos.” *Anatomy and Embryology* 150 (2): 171–186.

Christ, Bodo, and Beate Brand-Saberi. 2002. “Limb Muscle Development.” *International Journal of Developmental Biology* 46 (7): 905–914.

Cinnamon, Y., N. Kahane, and C. Kalcheim. 1999. “Characterization of the Early Development of Specific Hypaxial Muscles from the Ventrolateral Myotome.” *Development* 126 (19): 4305–4315.

Cook, M.J. 1965. *The Anatomy of the Laboratory Mouse*. London: Academic Press.

Cooke, J., and E.C. Zeeman. 1976. “A Clock and Wavefront Model for Control of the Number of Repeated Structures During Animal Morphogenesis.” *Journal of Theoretical Biology* 58 (2): 455–476.

Dale, J. Kim, Miguel Maroto, M.L. Dequéant, P. Malapert, M. McGrew, and Olivier Pourquié. 2003. “Periodic Notch Inhibition by Lunatic Fringe Underlies the Chick Segmentation Clock.” *Nature* 421: 275–278.

DeLaurier, A., N. Burton, M. Bennett, R. Baldock, D. Davidson, T. Mohun, and M. Logan. 2008. “The Mouse Limb Anatomy Atlas: An Interactive 3D Tool for Studying Embryonic Limb Patterning.” *BMC Developmental Biology* 8 (1): 83.

Deries, M., J.J.P. Collins, and M.J. Duxson. 2008. “The Mammalian Myotome: a Muscle with No Innervation.” *Evolution & Development* 10 (6): 746–755.

Deries, M., Ronen Schweitzer, and Marilyn J. Duxson. 2010. “Developmental Fate of the Mammalian Myotome - Deries - 2010 - Developmental Dynamics - Wiley Online Library.” *Developmental Dynamics* 239 (11): 2898–2910.

Dietrich, S. 1999. “Regulation of Hypaxial Muscle Development.” *Cell and Tissue Research* 296 (1): 175–182.

Dubrulle, Julien, and Olivier Pourquié. 2004. “Coupling Segmentation to Axis Formation.” *Development* 131: 5783–5793.

Dunwoodie, Sally. 2009. “Mutation of the Fucose-specific B1,3 N-acetylglucosaminyltransferase LFNG Results in Abnormal Formation of the Spine.” *Biochemica Et Biophysica Acta (BBA)- Molecular Basis of Disease* 1792 (2): 100–111.

Evrard, Yvonne, Yi Lun, Alexander Aulehla, Lin Gan, and Randy Johnson. 1998. “Lunatic Fringe: Is an Essential Mediator of Somite Segmentation and Patterning : Article : Nature.” *Letters to Nature* 394: 377–381.

Ferjentsik, Zoltan, Shinichi Hayashi, J. Kim Dale, Yasumasa Bessho, An Herreman, Bart De Strooper, Gonzalo del Monte, Jose Luis de la Pompa, and Miguel Maroto. 2009. “Notch Is a Critical Component of the Mouse Somitogenesis Oscillator and Is Essential for the Formation of the Somites.” Ed. Clarissa A. Henry. *PLoS Genetics* 5 (9) (September 25): e1000662. doi:10.1371/journal.pgen.1000662.

Fisher, R.E., H.F. Smith, K. Kusumi, E.E. Tassone, A. Rawls, and J. Wilson-Rawls. 2012. “Mutations in the Notch Pathway Alter the Patterning of Multifidus.” *The Anatomical Record: Advances in Integrative Anatomy and Evolutionary Biology*.

Fisher, Rebecca. 2011. “Illiocostalis Figures”. Unpublished Data, Personal Communication.

Greco, T L, S Takada, M M Newhouse, J A McMahon, A P McMahon, and S A Camper. 1996. “Analysis of the Vestigial Tail Mutation Demonstrates That Wnt-3a Gene Dosage Regulates Mouse Axial Development.” *Genes & Development* 10 (3) (February 1): 313–324. doi:10.1101/gad.10.3.313.

Gross, M.K., L. Moran-Rivard, T. Velasquez, M.N. Nakatsu, K. Jagla, and M. Goulding. 2000. “Lbx1 Is Required for Muscle Precursor Migration Along a Lateral Pathway into the Limb.” *Development* 127 (2): 413–424.

Haines, Nicole, and Kenneth Irvine. 2003. “Glycosylation Regulates Notch Signaling.” *Nature Reviews Molecular Cell Biology* 4: 786–799.

Hollway, G.E., and P.D. Currie. 2003. “Myotome Meanderings. Cellular Morphogenesis and the Making of Muscle.” *EMBO Reports* 4 (9): 855–860.

Hollway, Georgina, and Peter Currie. 2005. "Vertebrate Myotome Development." *Birth Defects Research Part C: Embryo Today: Reviews* 75 (3) (September): 172–179. doi:10.1002/bdrc.20046.

Ju, Bong-Gun, Sangyun Jeong, Eunkyung Bae, Seogang Hyun, Sean Carroll, Jeongbin Yim, and Jaeseob Kim. 2000. "Fringe Forms a Complex with Notch." *Nature* 405 (6783): 191–195.

Kablar, B., K. Krastel, C. Ying, A. Asakura, S.J. Tapscott, and M.A. Rudnicki. 1997. "MyoD and Myf-5 Differentially Regulate the Development of Limb Versus Trunk Skeletal Muscle." *Development* 124 (23): 4729–4738.

Kahane, N, C. Kalcheim, and Y. Cinnamon. 1998. "The Origin and Fate of Pioneer Myotomal Cells in the Avian Embryo." *Mechanisms of Development* 74 (1-2): 59–73.

Kahane, N., Y. Cinnamon, and C. Kalcheim. 1998. "The Cellular Mechanism by Which the Dermomyotome Contributes to the Second Wave of Myotome Development." *Development* 125 (21): 4259–4271.

Kalcheim, Chaya, and Raz Ben-Yair. 2005. "Cell Rearrangements During Development of the Somite and Its Derivatives." *Current Opinion in Genetics & Development* 15 (4) (August): 371–380. doi:10.1016/j.gde.2005.05.004.

Kardon, G., B.D. Harfe, and C.J. Tabin. 2003. "A Tcf4-positive Mesodermal Population Provides a Prepattern for Vertebrate Limb Muscle Patterning." *Developmental Cell* 5 (6): 937–944.

Kaufman, M.H. 1992. *The Atlas of Mouse Development*. London: Academic Press.

Kusumi, Kenro, and Sally Dunwoodie. 2010. *The Genetic and Development of Scoliosis*. New York Dordrecht Heidelberg London: Springer.

Lewis, J., A. Hanisch, M. Holder, and others. 2009. "Notch Signaling, the Segmentation Clock, and the Patterning of Vertebrate Somites." *J Biol* 8 (44): 11.

Lewis, Julian. 1998. "Notch Signalling and the Control of Cell Fate Choices in Vertebrates." *Seminars in Cell & Developmental Biology* 9 (6): 583–589.

Loomes, Kathleen M., Stacey A. Stevens, Megan L. O'Brien, Dorian M. Gonzalez, Matthew J. Ryan, Michelle Segalov, Nicholas J. Dormans, et al. 2007. "Dll3 andNotch1 Genetic Interactions Model Axial Segmental and Craniofacial Malformations of Human Birth Defects."

Developmental Dynamics 236 (10) (October): 2943–2951. doi:10.1002/dvdy.21296.

McClearn, D., R. Medville, and D. Noden. 1995. "Muscle Cell Death During the Development of Head and Neck Muscles in the Chick Embryo." *Developmental Dynamics* 202 (4): 365–377.

McGinnis, W, MS Levine, E Hafen, A Kuroiwa, and WJ Gehring. 1984. "A Conserved DNA Sequence in Homoeotic Genes of the Drosophila Antennapedia and Bithorax Complexes." *Nature* 308: 428–33.

Megeney, L A, B Kablar, K Garrett, J E Anderson, and M A Rudnicki. 1996. "MyoD Is Required for Myogenic Stem Cell Function in Adult Skeletal Muscle." *Genes & Development* 10 (10) (May 15): 1173–1183. doi:10.1101/gad.10.10.1173.

Morimoto, Mitsuru, Yu Takahashi, Maho Endo, and Yumiko Saga. 2005. "The Mesp2 Transcription Factor Establishes Segmental Borders by Suppressing Notch Activity." *Nature* 435: 354–359.

Murray, B., and DJ Wilson. 1997. "Muscle Patterning, Differentiation and Vascularisation in the Chick Wing Bud." *Journal of Anatomy* 190 (02): 261–273.

Nowicki, J.L., and A.C. Burke. 2000. "Hox Genes and Morphological Identity: Axial Versus Lateral Patterning in the Vertebrate Mesoderm." *Development* 127 (19): 4265–4275.

Nowiki, Julie. 2001. "Global Patterning of the Vertebrate Mesoderm: Interface Between Axial and Appendicular Muscluloskeltal Systems". Ph. D., University of North Carolina at Chapel Hill.

Ordahl, C.P., E. Berdougo, S.J. Venters, and WF Denetclaw. 2001. "The Dermomyotome Dorsomedial Lip Drives Growth and Morphogenesis of Both the Primary Myotome and Dermomyotome Epithelium." *Development* 128 (10): 1731–1744.

Ordahl, Charles, and Nicole Le Douarin. 1992. "Two Myogenic Lineages Within the Developing Somite." *Development* 114: 339–353.

Pourquié, O. 2001. "Vertebrate Somitogenesis." *Annual Review of Cell and Developmental Biology* 17: 311–50.

Pourquié, O. 2003. "The Segmentation Clock: Converting Embryonic Time into Spatial Pattern." *Science* 301 (5631): 328–330.

Pourquié, O. 2002. "Vertebrate Segmentation: Lunatic Transcriptional Regulation." *Current Biology* 12 (20): R699–R701.

Pownall, Mary Elizabeth, Marcus K. Gustafsson, and Charles P. Emerson. 2002. "Myogenic Regulatory Factors and the Specification of Muscle Progenitors in Vertebrate Embryos." *Annual Review of Cell and Developmental Biology* 18 (1) (November): 747–783. doi:10.1146/annurev.cellbio.18.012502.105758.

Pursglove, Sharon, and Joel Mackay. 2005. "CSL: A Notch Above the Rest." *The International Journal of Biochemistry & Cell Biology* 37 (12): 2472–2477.

Rawls, Alan, Julia Morris, Michael Rudnicki, Thomas Braun, Hans-Henning Arnold, William Klein, and Eric Olson. 1995. "Myogenin's Functions Do Not Overlap with Those of MyoD or Myf-5 During Mouse Embryogenesis." *Developmental Biology* 172 (1): 37–50.

Relaix, Frédéric, Didier Rocancourt, Ahmed Mansouri, and Margaret Buckingham. 2005. "A Pax3/Pax7-dependent Population of Skeletal Muscle Progenitor Cells." *Nature* 435 (7044) (April 20): 948–953. doi:10.1038/nature03594.

Ruiz-Gomez, M. 1998. "Muscle Patterning and Specification in Drosophila." *International Journal of Developmental Biology* 42: 283–290.

Saga, Yumiko, Haruhiko Koseki, N Hata, and M Taketo. 1997. "Mesp2: a Novel Mouse Gene Expressed in the Presegmented Mesoderm and Essential for Segmentation Initiation." *Genes & Development* 11: 1827–1839.

Sandow, A. 1970. "Skeletal Muscle." *Annual Review of Physiology* 32 (1): 87–138.

Sawada, Atsushi, Minori Shinya, Yun-Jin Jiang, Atsushi Kawakami, Atsushi Kuroiwa, and Hiroyuki Takeda. 2001. "Fgf/MAPK Signalling Is a Crucial Positional Cue in Somite Boundary Formation." *Development* 128: 4873–4880.

Serth, K. 2003. "Transcriptional Oscillation of Lunatic Fringe Is Essential for Somitogenesis." *Genes & Development* 17 (7) (April 1): 912–925. doi:10.1101/gad.250603.

Shifley, E. T., K. M. VanHorn, A. Perez-Balaguer, J. D. Franklin, M. Weinstein, and S. E. Cole. 2008. "Oscillatory Lunatic Fringe Activity Is Crucial for Segmentation of the Anterior but Not Posterior Skeleton." *Development* 135 (5) (January 30): 899–908. doi:10.1242/dev.006742.

Shifley, E.T. 2009. "The Regulation of Lunatic Fringe During Somitogenesis". The Ohio State University.

Sparrow, D.B., G. Chapman, M.A. Wouters, S. Ellard, D. Fatkin, P.D. Turnpenny, K. Kusumi, D. Sillence, and S. Dunwoodie. 2005. "Mutation of the LUNATIC FRINGE Gene in Humans Causes Spondylocostal Dysostosis with a Severe Vertebral Phenotype." *The American Journal of Human Genetics* 78: 28–37.

Stamataki, Despina, Maria-Christina Kastrinaki, Baljinder Mankoo, Vassilis Pachnis, and Domna Karagogeos. 2001. "Homeodomain Proteins Mox1 and Mox2 Associate with Pax1 and Pax3 Transcription Factors." *FEBS Letters* 499 (3): 274–278.

Stauber, Michael, Chetana Sachidanandan, Christina Morgenstern, and David Ish-Horowicz. 2009. "Differential Axial Requirements for Lunatic Fringe and Hes7 Transcription During Mouse Somitogenesis." Ed. Bruce Riley. *PLoS ONE* 4 (11) (November 24): e7996. doi:10.1371/journal.pone.0007996.

Stockdale, Frank. 1992. "Myogenic Cell Lineages." *Developmental Biology* 154: 284–298.

Takahashi, Yu, Atsuya Takagi, Shuichi Hiraoka, Haruhiko Koseki, Jun Kanno, Alan Rawls, and Yumiko Saga. 2007. "Transcription Factors Mesp2 and Paraxis Have Critical Roles in Axial Musculoskeletal Formation." *Developmental Dynamics* 236 (6) (June): 1484–1494. doi:10.1002/dvdy.21178.

Turnpenny, Peter D., Ben Alman, Alberto S. Cornier, Philip F. Giampietro, Amaka Offiah, Olivier Tassy, Olivier Pourquié, Kenro Kusumi, and Sally Dunwoodie. 2007. "Abnormal Vertebral Segmentation and the Notch Signaling Pathway in Man." *Developmental Dynamics* 236 (6) (June): 1456–1474. doi:10.1002/dvdy.21182.

Venters, S, and C Ordahl. 2002. "Persistent Myogenic Capacity of the Dermomyotome Dorsomedial Lip and Restriction of Myogenic Competence." *Development* 129: 3873–3885.

Weinmaster, Gerry, and Chris Kintner. 2003. "Modulation of Notch Signaling During Somitogenesis." *Annual Review of Cell and Developmental Biology* 19 (1) (November): 367–395. doi:10.1146/annurev.cellbio.19.111301.115434.

Wilson-Rawls, J., C.R. Hurt, S.M. Parsons, and A. Rawls. 1999. "Differential Regulation of Epaxial and Hypaxial Muscle Development by Paraxis." *Development* 126 (23): 5217–5229.

Wilson-Rawls, J., Jeffery Molkentin, Brian Black, and Eric Olson. 1999. "Activated Notch Inhibits Myogenic Activity of the MADS-Box Transcription Factor Myocyte Enhancer Factor 2C." *Molecular and Cellular Biology* 19 (4): 2853–2862.

Wu, J.Y., L. Wen, W.J. Zhang, and Y. Rao. 1996. "The Secreted Product of Xenopus Gene Lunatic Fringe, a Vertebrate Signaling Molecule." *Science* 273 (5273): 355–358.

Yamaguchi, TP, RA Conlon, and J Rossant. 1992. "Expression of the Fibroblast Growth Factor Receptor FGFR-1/flg During Gastrulation and Segmentation in the Mouse Embryo." *Developmental Biology* 152: 75–88.

Yu, Hslao-Man, Boris Jerchow, Tzong-Jen Sheu, Bo Liu, Frank Constantini, J. Edward Puzas, Walter Birchmeier, and Wei Hsu. 2005. "The Role of Axin2 in Calvarial Morphogenesis and Craniosynostosis." *Development* 132: 1995–2005.

Zhang, N, and T Gridley. 1998. "Defects in Somite Formation in Lunatic Fringe-deficient Mice." *Nature* 394: 374–377.